Department of Industrial Electrical Engineering and Automation

Magnetizing System

Ingemar Andersson

Supervisor: Mats Alaküla

21 December 2005

LUNDS TEKNISKA HÖGSKOLA
Lunds universitet

Abstract

Magnetization forces are one of the oldest known natural forces. Probably it was used in the early beginning of the history of man to perform some magical rituals. It is also one of the fundamental forces that affect us all the time by earth's polarisation. Perhaps it is related in some way to the force of gravity, but that will not be investigated in this thesis.

We have build up mathematical solutions to be able to calculate all the properties for magnetic forces. The stones that have this natural property is called magnetite, it is found in rocks and ore deposits. The shape is cubic, the colour is black and it glitters. It is often referred to as black ore and it is one of the most important ore deposits. Those materials have been magnetized by the earth's polarisation deep into the core when they weren't solid. The chemical sign is Fe_3O_4.

Materials can also be magnetized if an electric field is applied in the same direction as the desired. If this field is strong enough it will leave reminisce of magnetization in the material. This magnetization will be permanent and can be used in different applications. However, the magnetization will be decreased if the magnet is heated. When it cools down, the magnetization will increase again and eventually get its original magnetic flux. If it is heated to a temperature above a certain level called the Curie temperature it will be totally demagnetised, even if it cools down.

The thesis contents many different parts to meet its demands. The theoretical studies have at times been very comprehensive. This thesis expands over the parts of significance and a lot of the basic information is excluded.

This has been a very interesting thesis and for me it has given a loot of knowledge on the way, especially the practical construction part. Some parts are very absorbing and it has been necessary to not enter to deeply cause to the deadlines.

The thesis is written at a level that would equal master students knowledge, and to fully get the whole perspective, referrer to section 11(References).

Contents

1.Introduction

1.1Magnet properties

A permanent magnet will always have reminisced of field strength, called B. The amount of B has the unit Tesla. To make a magnet it is demanded that an electric field is applied, called H. The amount of H has the unit Amps/meter.

All materials have magnet properties but not all are suited for being permanent magnetized. It is the amount of valence electrons at the atom level that decide how well it will function, as well as the total amount of charge in the atoms has a major role. A dipole is an atom with electrons spinning around the core, building up a magnetic field because an electron could be seen as a current flow. The B field is a vector with 90° angles to the surface where the electrons are spinning. In non-magnetic materials those dipoles are randomly aligned. The dipoles are affecting the nearby atoms as well and therefore it is useful to portion an amount of atoms into a domain.

When an electric field H is applied the domains align with H and the result is a field B. As the H is decreasing the B will do the same and when H is zero hopefully it will remain a B field in the material, caused by those domains that remain in the forced position.

1.2 Magnetic calculations

From Gauss law for magnetism there's the fundamental expression

$$\oint BdA = 0 \tag{1.1}$$

.

A closed surface around a dipole will always have the resulting magnetic flux zero; cause to the B-field lines into the dipole will equal the lines out from the dipole. An area integral will thus result in the magnetic flux at the enclosed area.

$$\int B\cos\theta dA \Rightarrow \tag{1.2}$$

B perpendicular to the area

$$\Rightarrow \int BdA = \varnothing. \tag{1.3}$$

Combined with Faradays law for induction that substantiates that the change in area for a loop of wire inside a magnetic B-field corresponds to an induced voltage at the wire loop. The line integral in the equation can be seen as a wire loop.

$$E = ElectricField$$
$$\oint Eds = -\frac{d\varnothing}{dt} = -\frac{d(BA)}{dt}\left[Tesla*(m^2/s)\right] \tag{1.4}$$

If N is the number of turns this results in

$$V_{generated} = -N\frac{\Delta(BA)}{\Delta t} \tag{1.5}$$

Those two equations are fundamental and frequently referred to at the calculations in this thesis.

2. Problem formulation

An electrical motor is forced to rotate by magnetization forces, and the permanent magnets could either be placed on the outer surface of the rotor (normally AC machine) or at the inner surface of the stator (normally DC machine). The torque producing forces emanates from the permanent magnets interacting with the current flow in the windings of the motor. In an AC motor those forces is changing periodically, with the same speed as the frequency of the current. The local magnetization of the permanent magnets determines the forces. This magnetization needs to be well defined to minimize the power losses and give a smooth motion.

The permanent magnets around the motor are normally built up by loose magnets, which are placed around the case or the rotor like a ring. Another way is to make one magnet that is a solid ring. Those ring magnets is magnetized in one magnetic pulse and usually the result do not give a perfect amount of magnetic force in every point along the ring.

In this thesis a special type of magnetizing system will be developed that magnetizes a ring in separated magnetic pulses. Requirements on field strength in the air gap for magnetizing the ring are set to 4 Tesla. This system will emerge into a magnetizer prototype for ring magnets. It will go from idea to final result and it will include the practical construction, testing and running of the system.

When magnetizing a ring in the radius direction in a multipole pattern it is not possible to attain a field that sharply reverses at the transition region. This is due to the fields at the boundary that cancels each other out. If two magnetized parts are brought together they will affect each other's field as well. This effect is not negligible and the transition region is about 1.4 times the thickness of the ring.

3. Overview of the system

The magnetizing system consists of six major parts and a brief description will follow here. Figure 3.1.

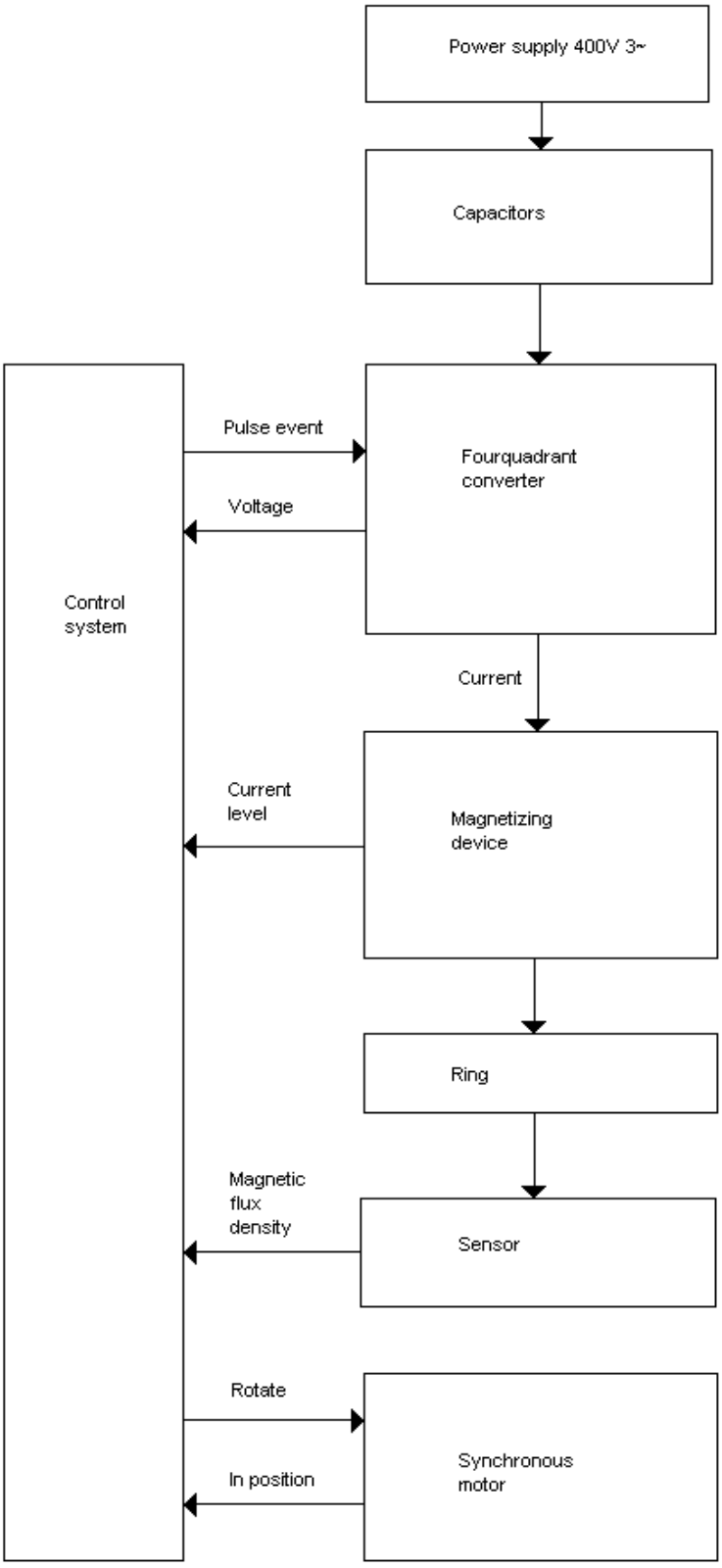

Figure 3.1: Magnetizing system.

The ring is placed on a synchronous motor that will rotate for one step at a time, whereas those steps could be for one degree on a 360° circle along the ring. When the ring is in position, the drive circuit has already built up the necessary amount of energy in its capacitors for the next magnetic pulse into the ring.

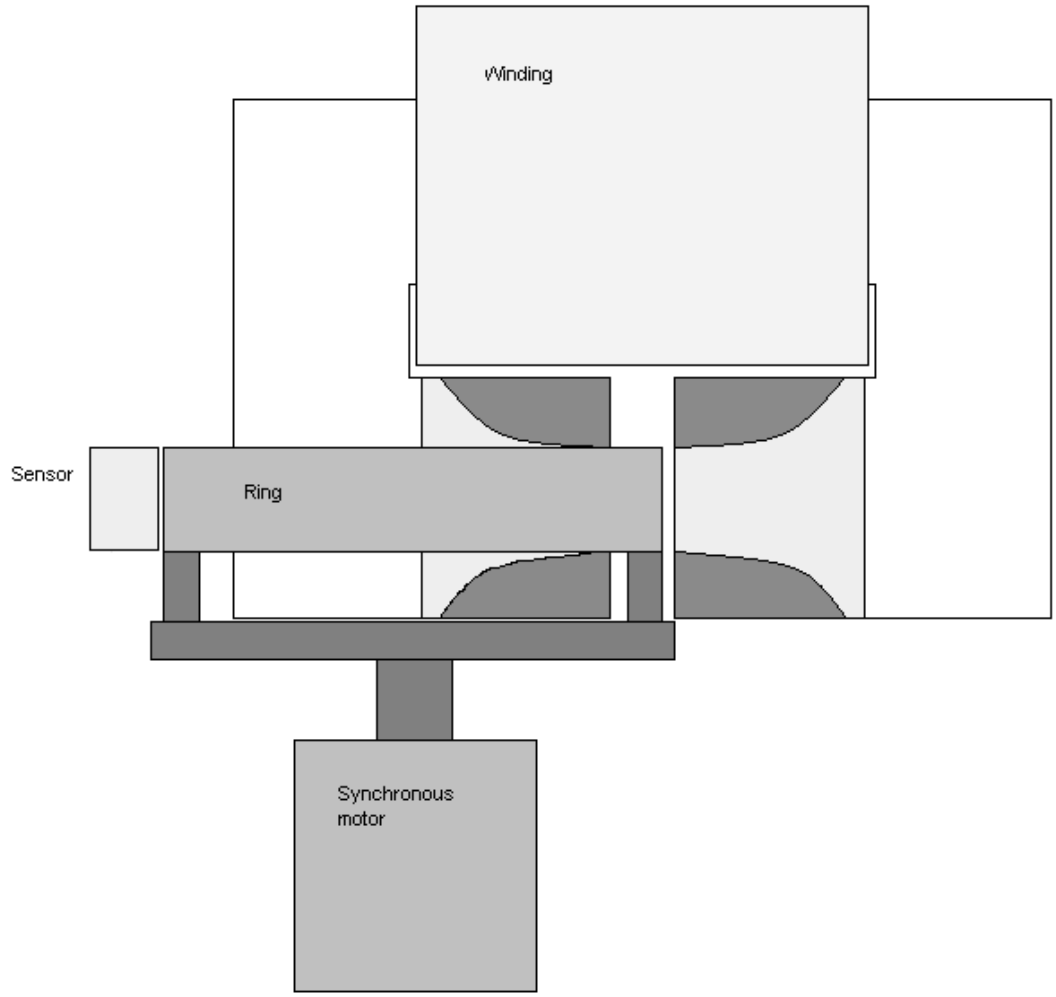

Figure 3.2: Magnetizing system.

The magnetic flux concentration has a high value at the air gap. The stated amount will be set to 4Tesla. A problem occurs cause to the iron properties at this amount; iron is saturated at approximately 2Tesla. When this event takes place the iron will behave like air, the effect is that the magnetic flux transports in all directions and the iron core have lost its purpose.

The idea to solve this problem is to force the magnetic flux into transporters and compress it. This lead to the presence of non saturated iron outside the transporters and highly saturated iron at the transporters with a very high resistance. The resistance will call for a high transporting force, which lead to a very high current pulse.

The ring receives a magnetic flux concentration that is compared to a sine wave. Passing parallel to the ring it can be read a pattern similar to a bar code.

The four-quadrant converter is supposed to do two magnetic pulses at each position at the ring. The first is to make as many domains as possible to align with the applied field and the other will be in the opposite direction and its purpose is to turn back those weak domains that are easy to align. The intention is that the strong domains will leave reminisces that corresponds to the wanted B field.

The magnetizing device transforms the current from the drive circuit to magnetic flow. The strength of B depends on the amount of current sent from the drive circuit to the magnetizing device.

A sensor registers the flux density at the magnetized ring, for calculation of the necessary amount of energy in the next magnetic pulse.

The calculations will be performed in the control system as well as all necessary function control. Calculations for the right amount of magnetic flux in the magnetic pulses shall also adapt to the material properties at the present ring placed in the device.

4. Synchronous motor

This motor will handle the movement of the ring. A step will be approximately a degree, depending on the diameter of the ring that is magnetized. The controlling device for the motor is not included in this thesis.

5. Magnetizing device

The magnetizing device consists of several materials and has been developed on the basis of a simulation program. The geometry for the magnetizing device is concluded from the theory that a magnetic field line always will be a closed loop. The coil current produces the magnetic field and the same field lines will enter the coil again.

An alternative to the construction could consist of two coils that would be placed mirrored relative each other and combined at the same air gap. This would decrease the amount of windings at each coil by half. The problem is the necessary of an opening to exchange the ring when it has been magnetized. It would also add some complexity to the solution for rotating the ring, since the possibility to place the ring on a rotating disk is excluded. Figure 5.1.

Another solution would be the emplacement of one coil at either end of the air gap. The length of the iron core would then increase and as seen later in this section, that would lead to increased resistance to the magnetic field. Figure 5.2.

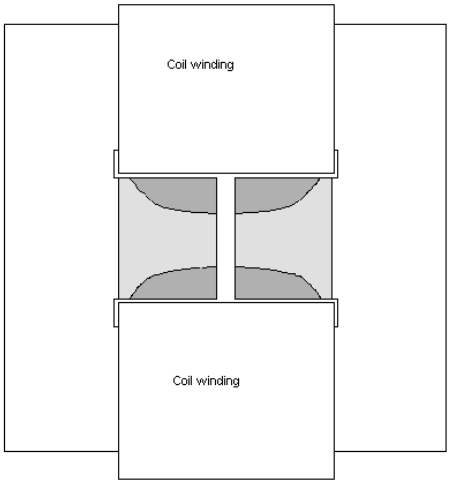

Figure 5.1 Alternative geometry.

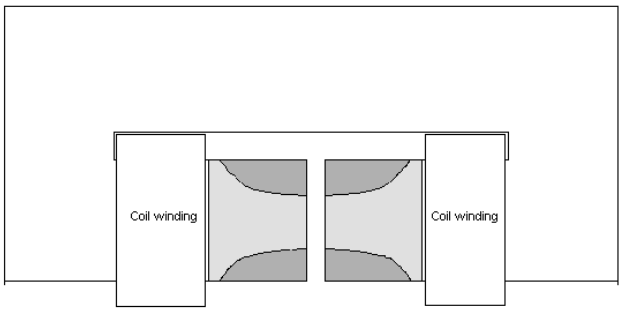

Figure 5.2 :Alternative geometry.

The selected geometry is shown in figure 5.3.

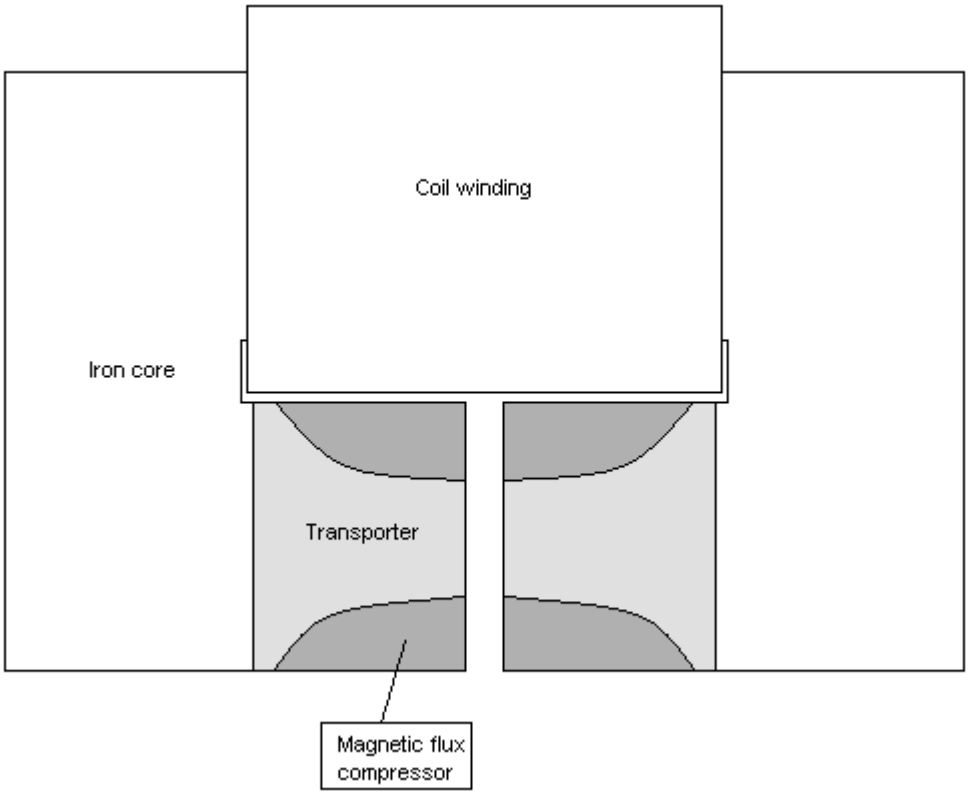

Figure 5.3: Selected geometry.

However, there are some fundamental characteristics for a magnets property.

$\phi = magneticflux[Weber]$

$N = turns$

$i = current[A]$

$\mu_{fe} = relativepermeability$

$\mu_0 = permeability(air)$

$l_{fe} = corelength$

$A_{fe} = corearea$

$\delta = airgapwidth$

$A_\delta = airgaparea$

$$\phi = \frac{N * i}{\frac{1}{\mu_{fe} * \mu_0} * \frac{l_{fe}}{A_{fe}} + \frac{1}{\mu_0} * \frac{\delta}{A_\delta}} \tag{5.1}$$

Those characteristics shows that the length of the magnet has to be as short as possible to get a large magnetic flux, nevertheless, the coil has to get the space needed to hold the number of turns. It is also necessary that the core area is large, as well as the relative permeability. Since the air gap area and air gap width is given and constant, the parameters we can adjustto adjust are the three earlier stated.

5.1 Simulation program

The program used for developing the device is called FEMM (FiniteElementMethodMagnets). This program is a quite powerful program for this purpose, even though it has its limitations. The way to conclude is to draw the magnet and setup material properties. Some of the materials will need their B-H curves to be stated. To view the simulation result, a program named FEMView is available inside FEMM.

5.1.1 FEMM

Geometry definitions can be entered manually in FEMM, but it is more convenient to use the built-in programming language Lua to read geometry definition commands from files, although FEMM only has a limited numbers of commands programmed. Programming in this language is similar to programming in the C-language. To make a smooth and fast way to setup a magnet for simulation, it has in this project been used Matlab to create and write a Lua file (Magnet.lua). The reason for this is that Matlab is able to calculate all given parameters and can be programmed to write the results together with Lua commands to a Lua file.

The file that Mat Lab uses, which has being created in this thesis, to calculate values for FEMM is named SetUpMagnetSom.m. To run this it is necessary to state a mount of different parameters. Table 5.1.

SetUpMagnetSom		
Parameter name (unit)	*Function*	*Used Value*
Width (cm)	Width inside device	7
Height (cm)	Height inside device	2.4
CoreSize (cm)	Cores height and width	11
GapTot (cm)	Total gap width between start points for slender	3
Gap (cm)	Width of air gap	0.4
RealCurrent (A)	Current trough windings	315
LaminationThickness (cm)	Iron core lamination thickness	0.015
InsulationBetweenLam (cm)	Iron core insulation thickness	0.001
CableArea (mm^2)	Cable winding area	9
FluxTransporterHeight (cm)	Height of air gap	0.4
TunnelWidht (cm)	Width for narrow tunnel section in somaloy at one side	0.4
SomaloyWidht (cm)	Width for somaloy block at one side	2.5
ArcShield (°)	Angle from GapTot to start of tunnel	60

Table 5.1: Stated parameters

When opening the created Magnet.lua file in FEMM the result is a designed magnet with stated parameters, although number of turns has to be stated manually. This value is 115 respectively -115. Figure 5.4.

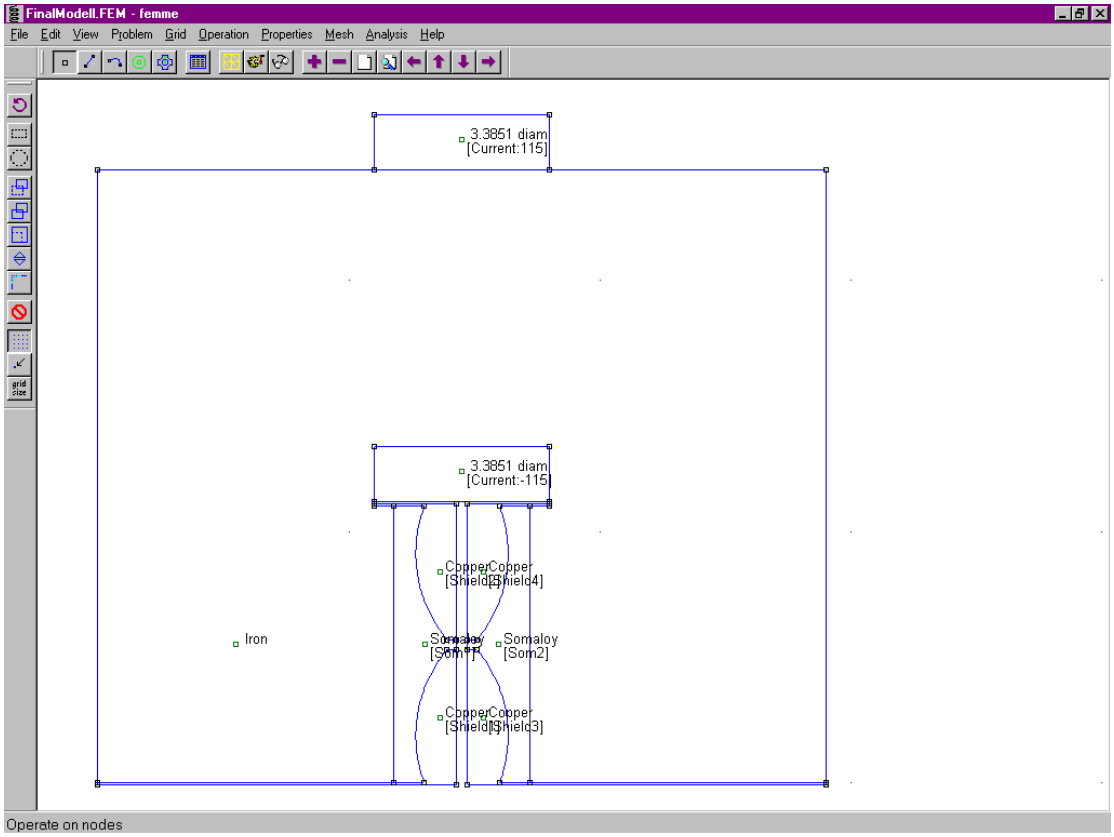

Figure 5.4: Drawn magnet

FEMM is a 2D analysis software, and can thus only be used to study two-dimensional properties. The depth can only be stated as a constant through the whole design. It is the height of the rotating ring in the air gap that will determine the stated depth. Otherwise the air gap area would have been increased and the result is a decreased reluctance. Therefore it will be necessary to recalculate the iron core design to get a quadratic shape when constructing the real magnetizing device. Further, the Somaloy transporters will become of a cone shape.

Before a simulation is performed it is compulsory to save the file as a .FEM-file. The simulation is executed by pressing the handle at the tool bar in the FEMM window.

5.1.2 FEMView

After a FEM calculation has been finished the FEMView is started for post processing, i.e. to study the flux density, forces etc that are relevant results. There are several useful tools for evaluation; one of these is circuit property. This tool shows all relevant information about the coil, such as voltage drop, inductance etc. Figure 5.5.

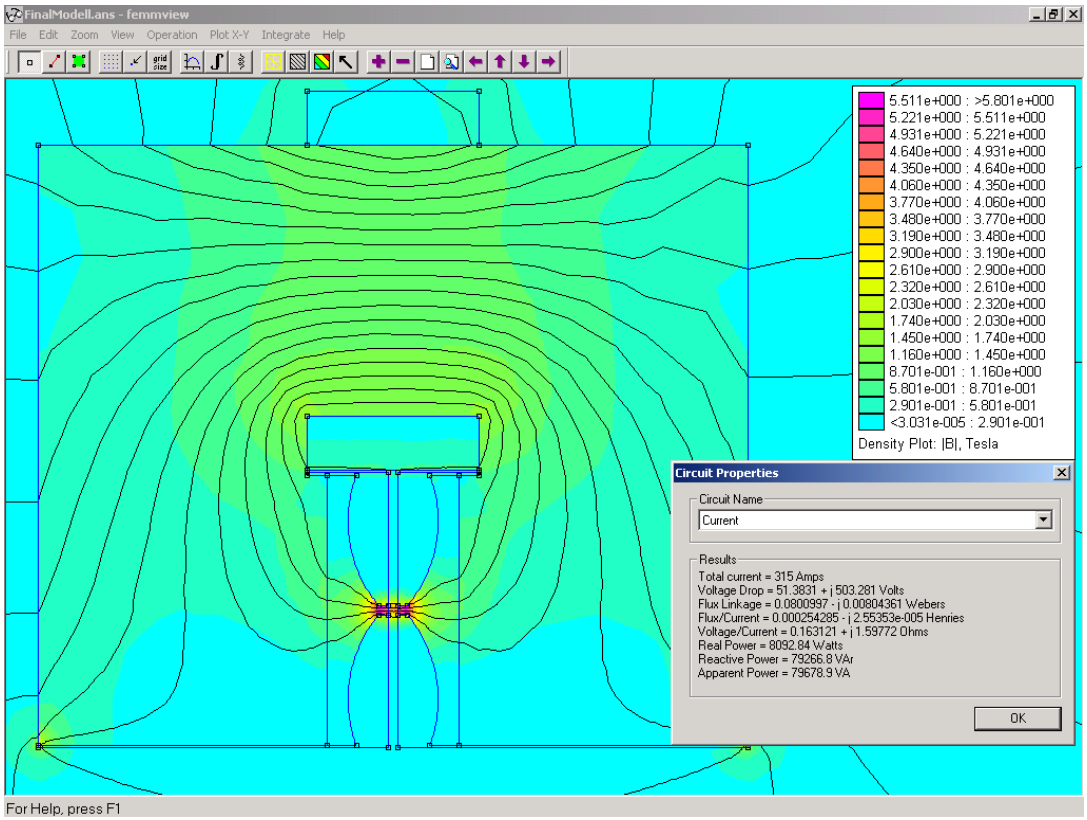

Figure 5.5: Magnet after simulation.

The most interesting part is the air gap where the ring is to be placed. Any part could be highlighted and enlarged. The concentration of B-field is seen to have strength 4 Tesla at the centre of the air gap. Figure 5.6.

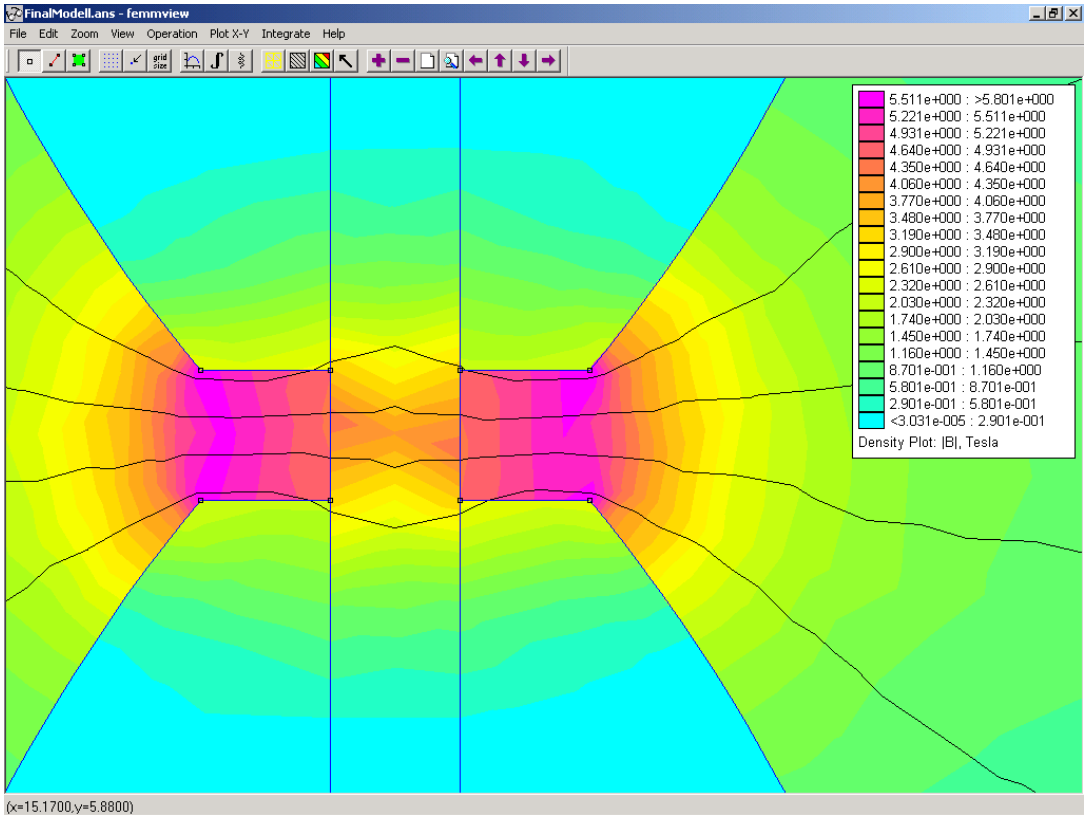

Figure 5.6: Air gap.

The purpose of the tunnel part just before air gap where the area is constant is to concentrate the field strength as much as possible.

Along a straight line placed in the centre of the air gap, perpendicular to the B-field, the field concentration can be seen to have a sharp distribution. Figure 5.7. The ideal shape of this curve had been a square wave. The air gap has a length of 4 mm and the concentration is fairly high outside the gap as well. A problem occurs when a magnetic pulse is done, the B-field will also affect the nearby regions at the ring, which maybe already had been magnetized. The control system is nevertheless adaptive and this could in some way take care of this diffusion.

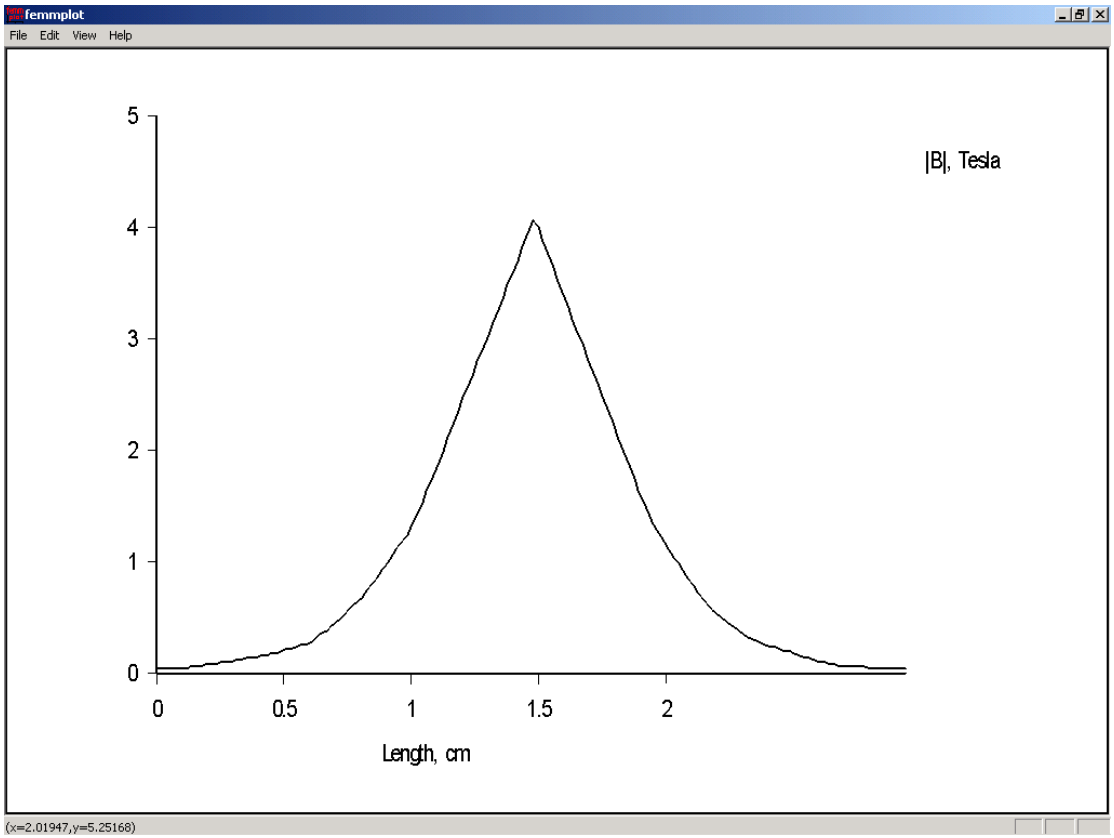

Figure 5.7: Magnetic flux density in air gap.

5.2 Material properties

There are three different materials in the magnetizer device and their properties will be explained here.

5.2.1 Copper

Copper has been placed around the Somaloy at the air gap. Reason for placement here is that copper is a good conduction material and that eddy currents will be excited, which prevents magnetic flux penetration and thus helps focusing the flux. Eddy currents would completely eliminate the magnetic flux if it could pass around the field flow. Therefore the copper has been split into four parts, with insulation between. Eddy current will only appear if the B-field is changing and at this device the demands that the field could be steered into the air gap is very high. To get a satisfied concentration in magnetic flux, the frequency of the pulse has to be as high as 1 kHz.

5.2.2 Somaloy™ 500

Somaloy ™ 500 has been used for the parts that transports magnetic flow from iron core to air gap. A reason for having this material is that the switching losses will decrease; due to the low conductance in Somaloy™ 500. This part is furthermore not laminated, since field lines shall transfer in three dimensions. Figure 5.8.

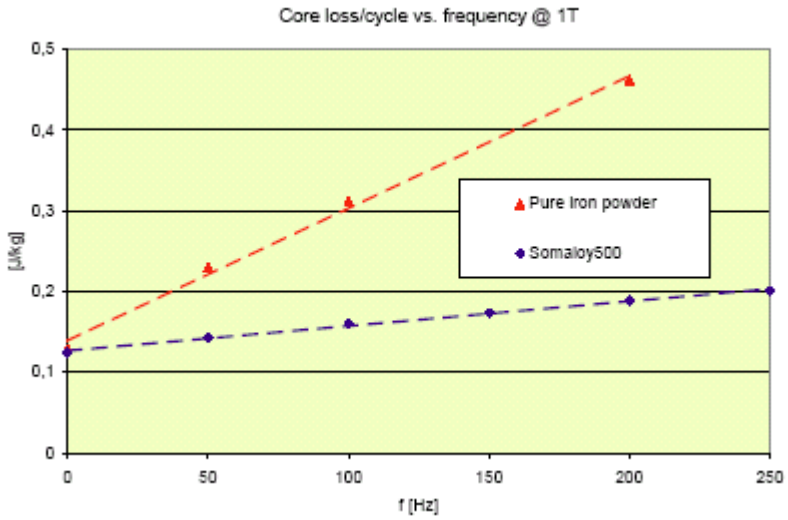

Figure 5.8: Switching losses for iron and Somaloy. [1]

Somaloy is a special designed material to have high resistance as well as high density. It consists of compressed iron powder but it has instead a thinner insulation layer between each particle than in normally compressed magnet material. A special lubricant called Kenolube™ is developed at Höganäs AB Sweden, with property of a strong tenability protection layer. Figure 5.9.

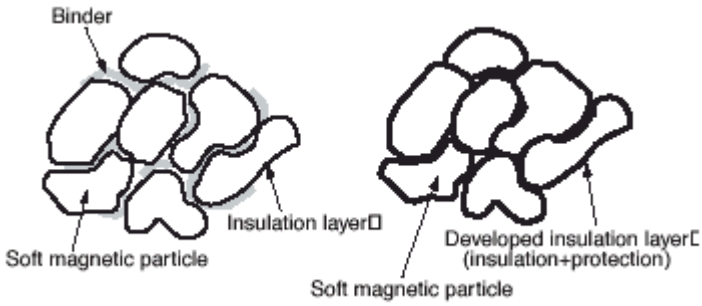

Figure 5.9: Particle composition. [8]

The higher resistance contribute to lower switching losses at medium frequencies, cause to lower eddy currents that otherwise would oppose the applied field. The high density contribute to the total amount of air gap in the material will be decreased, which will result in better magnetic flux conductivity.

The Somaloy™ 500 B-H curve used at the simulations is shown in figure 5.10.

5.2.3 Iron core

Laminated iron is used in most of the core material at the magnetizing device. It is used in those parts where there is no saturation of magnetic flux. Nevertheless, there are eddy currents caused by the pulse, the iron is a fully satisfied material to use here. The lamination in this part is fairly thin so these eddy current will be acceptable small. When eddy current is passing in opposite directions along both sides of lamination, they will oppose each other by the appearance of there own B-fields.

The laminated iron and Somaloy500 B-H curves used at the simulations are shown in figure 5.8. The iron is laminated and able to transport magnetic field in two dimensions therefore it will get a higher value for the B-field in those directions, whereas the Somaloy500 is solid and able to transport magnetic field in a three dimensional space.

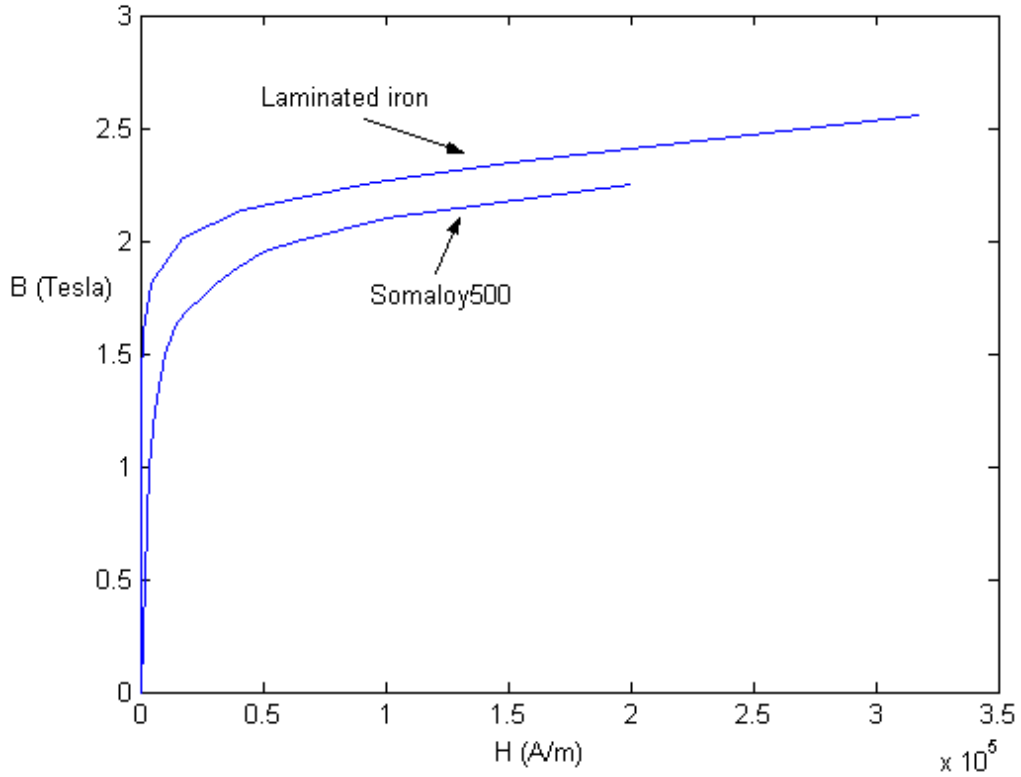

Figure 5.10: B-H properties for laminated iron and Somaloy500.

5.3 Power calculations

When searching for a device that will encounter the demands that is set up for application, it is lengthy to count all parameters by hand. This application that has several material and furthermore transporters that will steer B-field to a slender air gap could be very time demanding to calculate. The way to conclude is by trying different simulations and amends the device in front of following simulations.

Calculations for control of the given values by FEMView has nevertheless been necessary to perform, despite of the advantage with a program like this.

The calculated values by FEMView at the magnetizing device circuit are represented in table 5.2 and they are also represented in figure 5.11.

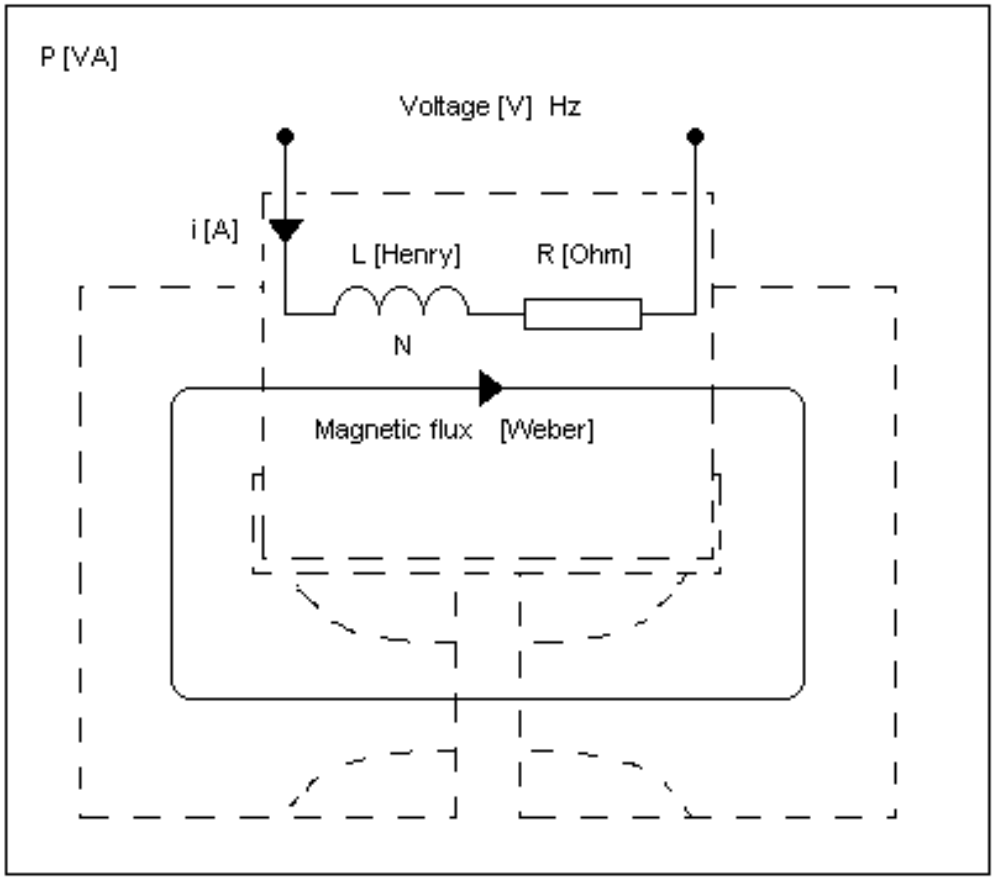

Figure 5.11: Circuit geometry.

Type	Value	Unit	Symbol
Total current	315	Amps	i
Voltage Drop	51.3831 + j 503.281	Volts	V
Flux/Current	0.000254285 - j 2.55353e - 005	Henries	L
Voltage/Current	0.163121 + j 1.59772	Ω (Ohms)	R
Apparent Power	79678.9	VA	P
Flux Linkage	0.0800997 - j 0.00804361	Webers	ϕ
Number of turns	115	quantity	N
Frequency	1000	Hertz	Hz

Table 5.2: Circuit properties.

Further, the voltage is a sine wave that is performed as a pulse for each magnetizing session. This pulse drives a current pulse for 315 A, and finally the current pulse give raise to the magnetic flux. Those two latter signals will be similar to a sine wave but they will probably be deformed cause to different properties at the materials of the

magnetizing device. Achieving the right amount of current is the essential goal; the importance of a perfect sine wave is ignored.

It is also necessary to be able to magnetize in the opposite direction, applying a negative voltage attains this.

5.3.1 Inductance

Inductance of the coil is calculated with these formulas:

$$\left.\begin{aligned} u_L &= L * \frac{di}{dt} \\ e = u_L &= \frac{d\phi}{dt} * N \end{aligned}\right\} \Rightarrow L * \frac{di}{dt} = \frac{d\phi}{dt} * N \Rightarrow L = \frac{d\phi}{di} * N \tag{5.2}$$

$$\left.\begin{aligned} i &= \hat{i} * \sin(\omega t - \varphi) \\ \frac{di}{dt} &= \omega \hat{i} * \cos(\omega t - \varphi) \\ di &= \omega \hat{i} * \cos(\omega t - \varphi) dt \end{aligned}\right\} \tag{5.3}$$

$$\left.\begin{aligned} \phi &= \hat{\phi} * \sin(\omega t - \varphi) \\ \frac{d\phi}{dt} &= \omega \hat{\phi} * \cos(\omega t - \varphi) \\ d\phi &= \omega \hat{\phi} * \cos(\omega t - \varphi) dt \end{aligned}\right\} \tag{5.4}$$

$$L = \frac{d\phi}{di} * N = \frac{\omega \hat{\phi} * \cos(\omega t - \varphi) dt}{\omega \hat{i} * \cos(\omega t - \varphi) dt} * N = \frac{\hat{\phi}}{\hat{i}} * N \tag{5.5}$$

$\omega = 2\pi f$

$\hat{i} = 315A$

$\hat{\phi} = B * A[Weber]$

$L = induc\tan ce[H]$

N = number of turns=115

B = B-field concentration

A = area of the core

One way to approach the value for the magnetic flux through the coil is to plot the generated B-field concentration in the part of iron core that is placed inside the coil. Figure 5.12.

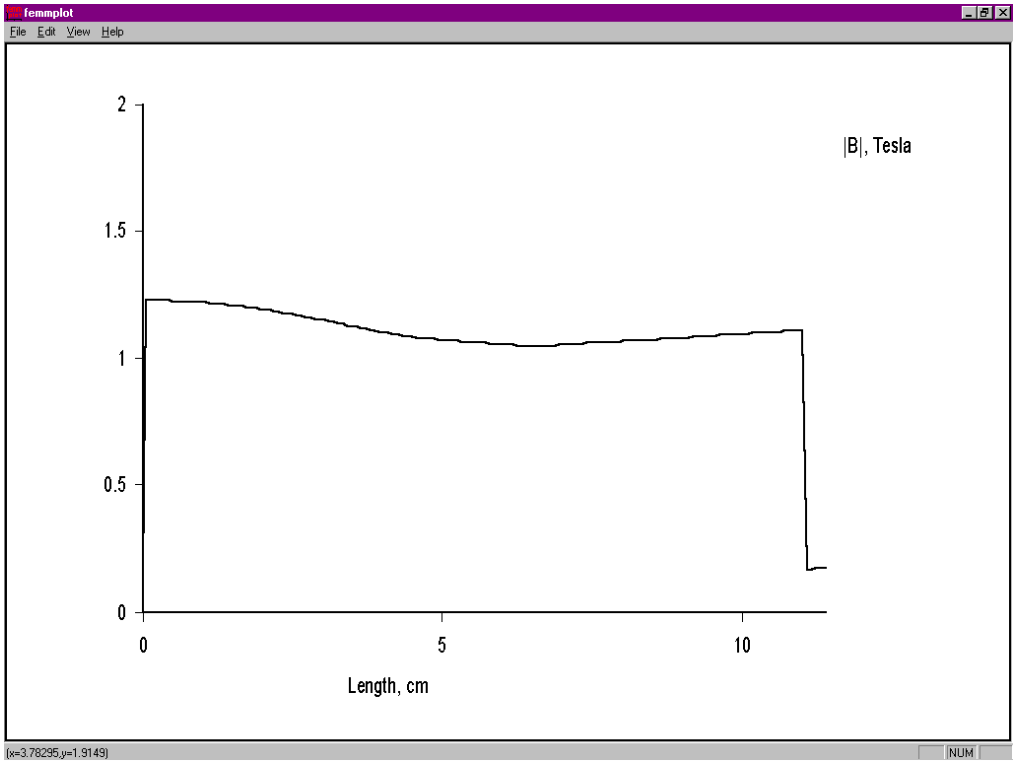

Figure 5.12: Magnetic flux density at iron core.

The B-field has an approximated average concentration of 1.1 Tesla and the area is

$$0.11m * 0.006m = 0.66 * 10^{-4} m^2 \tag{5.6}$$

which leads to

$$\hat{\phi}_{Calculated} = B * A = 1.1 * 0.66 * 10^{-4} = 0.73mWeber$$

$$\hat{\phi}_{FEMView} = \frac{|\text{Flux Linkage}|}{\text{N}} = \frac{|\psi_{FEMView}|}{N} = \frac{|0.0800997 - j\,0.00804361|}{115} = \frac{0.081}{115} = 0.70mWeber \tag{5.7}$$

$$L_{Calculated} = \frac{\hat{\phi}}{\hat{i}} * N = \frac{0.73m}{315} * 115 = 0.27mH \tag{5.8}$$

$$L_{FEMView} = \frac{\hat{\phi}}{\hat{i}} * N = \frac{0.70m}{315} * 115 = 0.26mH \tag{5.9}$$

.

Comparing this value with the given inductance value by FEMView

$$L_{FEMViewGiven} = \text{Flux/Current} = 0.000254285 - j\,2.55353e-005 \text{ Henries} \tag{5.10}$$

$$|L_{FEMViewGiven}| = 0.26mH \tag{5.11}$$

$$L_{Calculated} = 0.27mH \tag{5.12}$$

gives a satisfying result, and the flux function is determined to be

$$\phi(t) = \hat{\phi} * \sin(\omega t - \varphi) = 0.70m * \sin(2\pi 1000t - \varphi) \tag{5.13}$$

5.3.2 Current

The current is by simulations determined to 315A. Since this is the value that generates the received B-field in the magnetizing device, it is also the current peak value. However, current has a lag angle compared to the voltage. This lag angle is taken straightforward from the given values from FEMView. It is likely though that the angle should be almost 90° since the load is almost completely inductive.

$\hat{i} = 315A$

$\omega = 2\pi 1000$

$u(t) = \hat{u} * \sin(\omega t)$ (5.14)

$i(t) = \hat{i} * \sin(\omega t - \varphi)$ (5.15)

$$\tan\varphi = \frac{\mathrm{Re}\,activePower}{\mathrm{Re}\,alPower} = \frac{79266.8}{8092.8} \quad (5.16)$$

$$\varphi = 84.2° \Leftrightarrow \varphi = \frac{47\pi}{100} \quad (5.17)$$

$$i(t) = \hat{i} * \sin(\omega t - \frac{47\pi}{100}) \quad (5.18)$$

The current will have a function similar to

$$i(t) = 315 * \sin(2\pi 1000t - \frac{47\pi}{100}) \quad (5.19)$$

5.3.3 Voltage

The voltage drop across the coil can be calculated by utilization of the following equations. The calculated values will be compared with the given by FEMView for determination of the definitive voltage.

$$u_L = L * \frac{di}{dt} = L * \omega * \hat{i} * \cos(\omega t - \varphi) \quad (5.20)$$

$$e = u_L = N * \frac{d\varphi}{dt} = N * \omega * \hat{\phi} * \cos(\omega t - \varphi) \quad (5.21)$$

$L_{FEMView} = 0.26mH$

$L_{Calculated} = 0.27mH$

$\omega = 2\pi 1000$

$\hat{i} = 315A$

$N = 115$

$\hat{\phi} = 0.70mWeber$

$\varphi = \frac{47\pi}{100}$

The voltage top value is the value of interest, therefore the amplitudes in 5.20 and 5.21 are calculated.

$$u_{L,FEMView}(L = 0.26mH) = 0.26m * (2\pi 1000) * 315 = 515V \quad (5.22)$$

$$u_{L,Calculated}(t = 0.27mH) = 0.27m * (2\pi 1000) * 315 = 534V \quad (5.23)$$

$$e_{\hat{\varphi},FEMView}(t = 0.24) = 115 * (2\pi 1000) * 0.70m = 506V \quad (5.24)$$

The given value by FEMView is

$$\text{Voltage Drop} = 51.3831 + \text{j}\,503.281 \text{ Volts}$$

$$|\text{Voltage Drop}| = 506 \text{ Volts} \quad (5.25)$$

The voltage is finally determined to

$$Voltage_{average} = \hat{u} = \frac{515 + 534 + 506}{3} \approx 518V \quad (5.26)$$

.

Therefore the voltage function is

$$u = \hat{u} * \sin(\omega t) = 518 * \sin(2\pi 1000t) \quad (5.27)$$

5.3.4 Conclusions

The three stated functions for voltage, current and magnetic flux.

$$u(t) = 518 * \sin(2\pi 1000t) \quad (5.27)$$

$$i(t) = 315 * \sin(2\pi 1000t - \frac{47\pi}{100}) \quad (5.19)$$

$$\phi(t) = 0.70m * \sin(2\pi 1000t - \frac{47\pi}{100}) \quad (5.13)$$

The plot of the functions determines how long time the voltage has to be controlled. Time is 0.24 to 0.74ms, and the purpose is to steer down the current pulse to zero again. 1M at the plot multiply the flux. Figure 5.12.

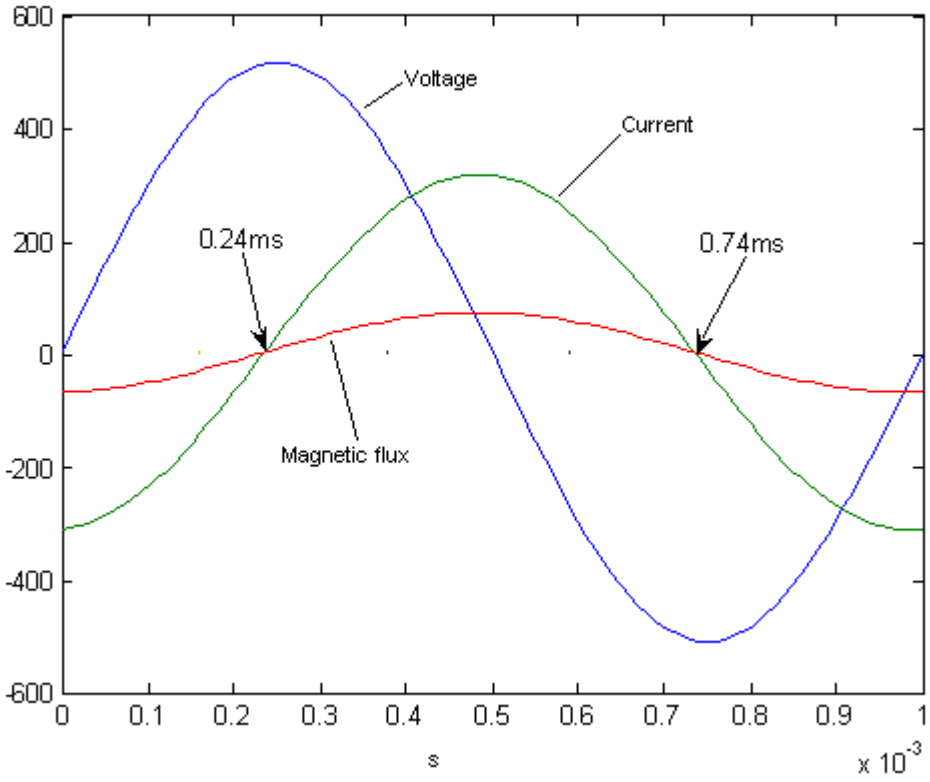

Figure 5.12: Voltage, current and magnetic flux.

5.4. Drawing of the magnetizing device

A drawing of the final model of the device is shown in fig 5.13. There are four copper parts per Somaloy transporter. All these parts have to be varnished to be electrically isolated from each other. Fitting together those parts is important, due to air between the Somaloy and the copper has a decreasing effect on the magnetic flux conductivity.

The Somaloy transporters are shown in fig 5.14.

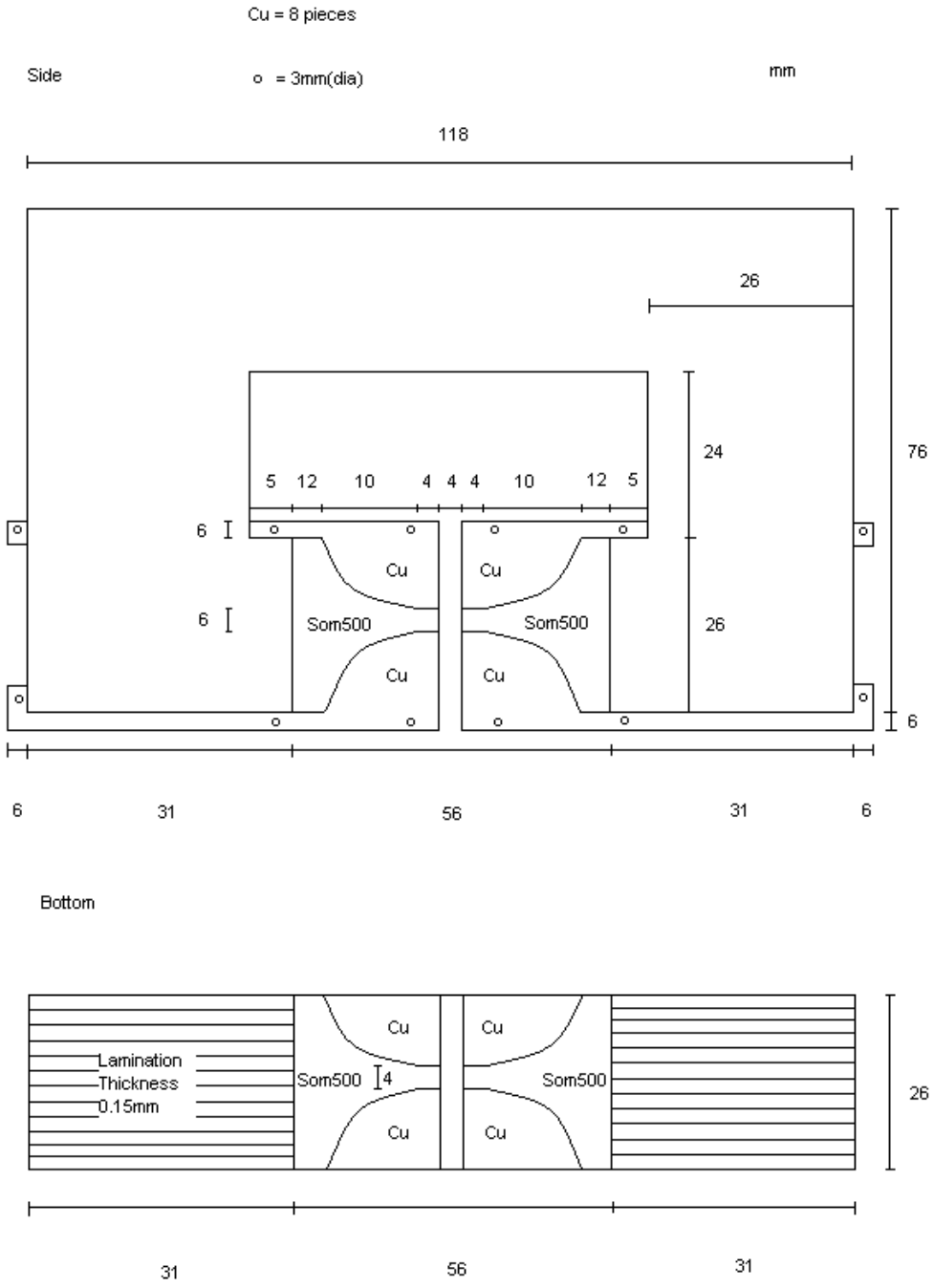

Figure 5.13: Magnetizing device.

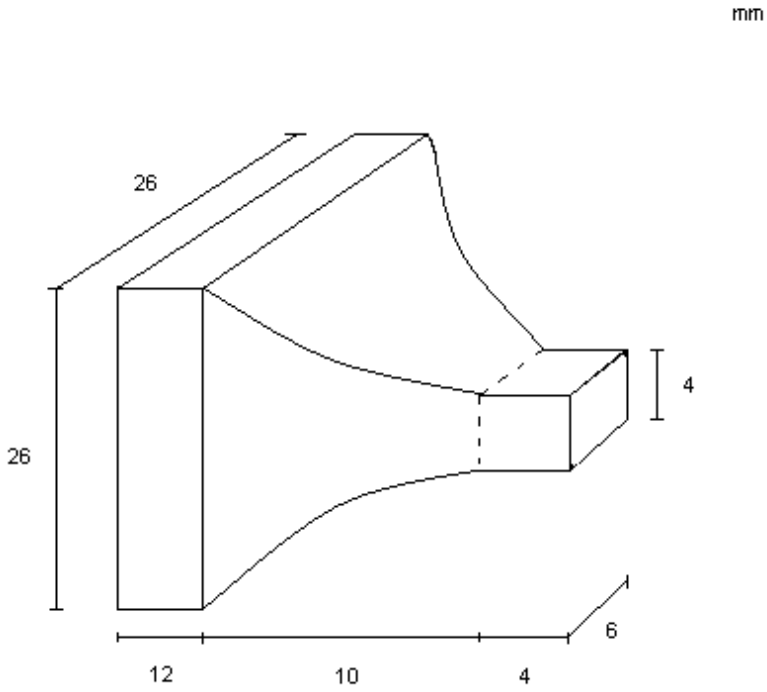

Figure 5.14: Somaloy transporter.

To hold the device together when it is in operation there has to be plastic plates that is screwed together at both sides of the transporters. The forces can be very high so this material is preferred as fibreglass. Figure 5.15.

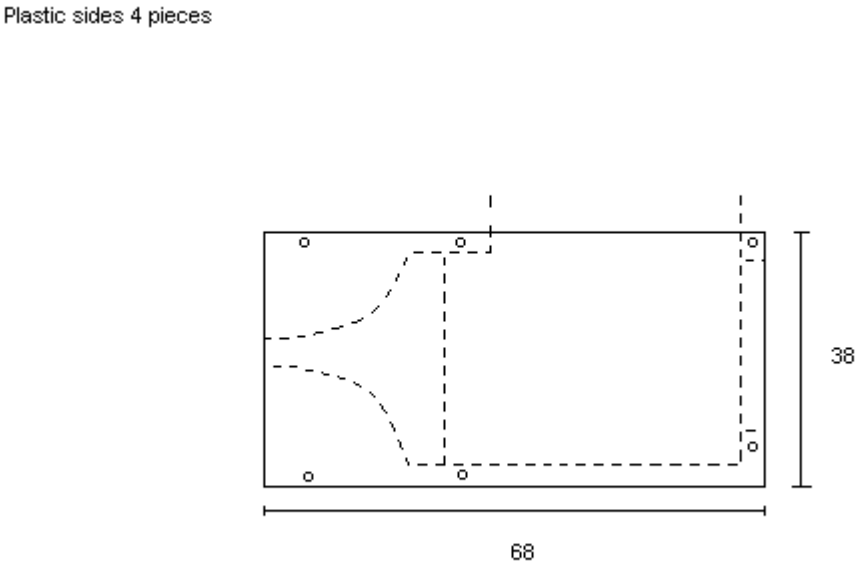

Figure 5.15: Plastic plates.

6. Power electronics

The power electronics consists of a four-quadrant converter, capacitors, driver and a three-phase rectifier. Figure 6.1. Since the requirement that the ring has to be magnetized in two different directions, it is needed that the current can be bi-polar, thus the 4-quadrant converter. This device is able to steer the current through the magnetizing device in either positive or negative direction. A requirement is also that the voltage shall change polarity in each magnetic pulse; this property is required to control the pulse at the negative slope. The capacitors will charge the amount of energy needed in front of each magnetic pulse. To protect the rectifier from the charge current rush to the capacitors direct after a magnetic pulse, a protective coil will be placed between the rectifier and the capacitors. The protective coil is further explained in section 6.5.

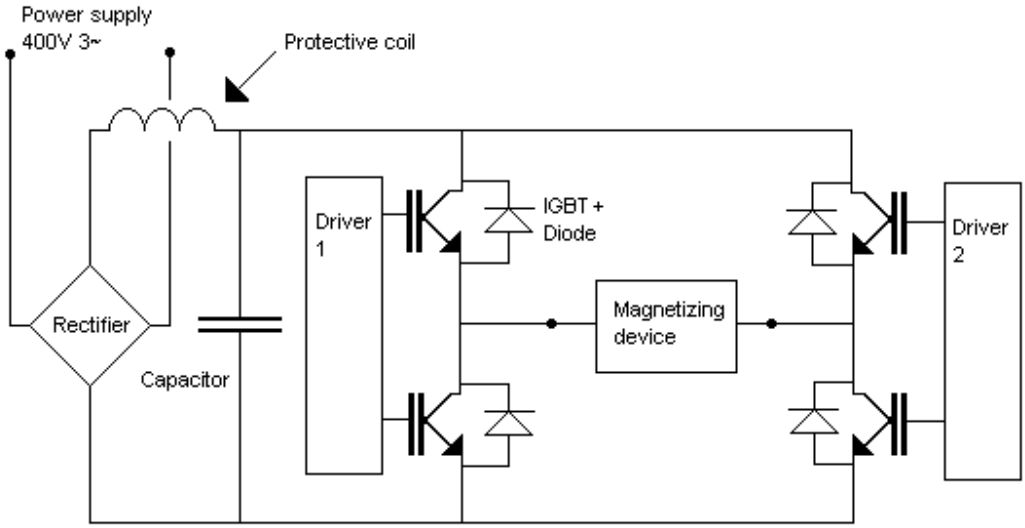

Figure 6.1:Power electronics.

Three phase supply voltage will give a specific dc-link voltage, which is initially determined with consideration to the totally capacitive dc-link.

$$u_1 = 565 * \sin(wt) \tag{6.1}$$

$$u_2 = 565 * \sin(wt - \frac{2\pi}{3}) \tag{6.2}$$

$$u_3 = 565 * \sin(wt - \frac{4\pi}{3}) \tag{6.3}$$

DC-link voltage

$$V_{DC} = \frac{3\sqrt{2}}{\pi} E_{LL} = \frac{3\sqrt{2}}{\pi} 400 = 540V \tag{6.4}$$

.

It is advantageous to have more than ten switchings per pulse

$$f_{sw} = 10 * 1000Hz = 10kHz \tag{6.5}$$

However, it's advantageous to maximize the switching frequency. Higher frequency gives a better control of the current to the magnetization device. Therefore it will, as seen later in this document, be maximized depending on the driver.

6.1 Four-quadrant converter

The Four-quadrant converter consists of four IGBT: s and four freewheeling diodes. When it is conducting current, equal to two IGBT: s is open, then the freewheeling diodes are blocked. The freewheeling diodes will conduct at the moment the IGBT: s is closing. The purpose is to lead the current that builds up inside the coil when the IGBT: s is conducting.

IGBT Safety margins:

$$I_{C(125°C)} > \frac{\hat{i}}{0.8} = \frac{305}{0.8} = 381.3A \tag{6.6}$$

$$V_{CES} > \frac{V_{DC}}{0.6} = \frac{540}{0.6} = 900V \tag{6.7}$$

Where the safety margin is 80% respectively 60% of the maximum current flow and the voltage across the IGBT:s from the datasheets. Therefore the increasing dividers of 0.8 and 0.6 have been used.

Suitable transistor half bridge is SKM400GB128D from Semikron:

$V_{CES} = 1200V$
$I_C = 400A$
$f_{SW} = 20kHz$
$V_{GE} = \pm 15V$

A necessary parameter to reflect on already on this state is the amount of charge (Q_G) that the IGBT: s demands. The minimum amount of charge times the switching frequency gives the average current that the driver has to deliver. This parameter is necessary to calculate at this state because the switching frequency decides the switching losses for the IGBT: s.

The selected driver is constructed to deliver a maximum average current of 50mA (I_{GAV}). The driver is evaluated in section 6.2.

[5](Fig.6, p.390):

$$V_{GE} = 15V \Rightarrow Q_G = 2900nC \Rightarrow I_{GAV} = f_{sw} * Q_G = 17k * 2900n = 4.9mA \tag{6.8}$$

Therefore, the switching frequency will be stated to:

$$f_{sw} = 17kHz \tag{6.9}$$

This is the maximum switching frequency that is limited by the driver gate charge delivery.

6.1.1 Switching losses

When encountering the demands for cooling and maximum working temperature, it is important to calculate the switching losses. The consequences of negligating this effect may be incalculable. When searching for the value for each swithing it is necessary to read the data sheets carefully. The values is found in different tables. [5](Fig.4, p.390):

$E_{on} = 20mJ$

$E_{off} = 32mJ$

$E_{rr} = 20mJ$

$V_{CC} = 600V$

$I_C = 300A$

$I_0 = I_{dc} = 315A$

$V_{dc} = 540V$

Finding the values and inserting in the following equations, where the losses in Joule times the frequency results in power losses $\left(\frac{J}{s} = W\right)$.

Where

$P_{Tsw} = Switching\ losses, IGBT$

$P_{Dsw} = Switching\ losses, diode$

$P_{Tcond} = Conduction\ losses, IGBT$

$P_{Dcond} = Conduction\ losses, diode$

$$P_{Tsw} = f_{sw} * (E_{on} + E_{off}) = 17k * (20m + 32m) = 884W \quad (6.10)$$

$$P_{Dsw} = \frac{2*\sqrt{2}}{\pi} * \frac{E_{rr}}{V_{CC} * I_C} * V_{dc} * I_{dc} * f_{sw} = \frac{2*\sqrt{2}}{\pi} * \frac{20m}{600*300} * 540 * 315 * 17k = 289W \quad (6.11)$$

$$P_{Tcond} = \left(\frac{\sqrt{2}}{\pi} * V_{CE(T0)} * I_0 + \frac{1}{2} * r_{CE} * I_0^2\right) + \left((V_{CE(T0)} * I_0 * \frac{4\sqrt{2}}{3\pi} * r_{CE} * I_0^2\right) \frac{U_0 * \cos(\varphi)}{V_{dc}} \quad (6.12)$$

$$P_{Tcond} = \left(\frac{\sqrt{2}}{\pi} * 1.15V * 315A + \frac{1}{2} * 5m\Omega * (315A)^2\right) + 0 = 411W \quad (6.13)$$

$$P_{Dcond} = \left(\frac{\sqrt{2}}{\pi} * V_{(T0)} * I_0 + \frac{1}{2} * r_T * I_0^2\right) - \left((V_{(T0)} * I_0 * \frac{4\sqrt{2}}{3\pi} * r_T * I_0^2\right) \frac{U_0 * \cos(\varphi)}{V_{dc}} \quad (6.14)$$

$$P_{Dcond} = \left(\frac{\sqrt{2}}{\pi} * 1.2V * 315A + \frac{1}{2} * 4.3m\Omega * (315A)^2\right) - 0 = 383W \quad (6.15)$$

$$P_T = P_{Tsw} + P_{Tcond} = 884W + 411W = 1295W \quad (6.16)$$

$$P_D = P_{Dsw} + P_{Dcond} = 289W + 383W = 672W \quad (6.17)$$

This result is the power losses at the IGBT:s.

6.2 Driver

As stated earlier the switching frequency will be 17kHz. With this frequency related to the pulse frequency, there will be

$$\frac{17k}{1k} = 17\frac{switchings}{period} \tag{6.18}$$

.

A suitable driver is SKHI 23/17:

To get the calculated losses in Chapter 6.1, the gate resistor (R_{Gate}) has to be approximately 4.7 Ω. [5](Fig.4, p.390). The built in resistor in the driver with 22 Ω has to be parallel connected by a resistor with value 6 Ω.

$$\frac{R_{parallel} * R_{builtin}}{R_{parallel} + R_{builtin}} = 4.7\Omega \tag{6.19}$$

$$R_{builtin} = 22\Omega$$

$$R_{parallel} = \frac{4.7 * R_{builtin}}{R_{builtin} - 4.7} = \frac{4.7 * 22}{22 - 4.7} = 6\Omega \tag{6.20}$$

This is not exceeding the $I_{OUTpeak}$ value at the driver stated as 8A. ([5], p.1949).

$$I_{OUT} = \frac{V_{CE}}{R_{Gate}} = \frac{15V}{4.7\Omega} = 3.2A \tag{6.21}$$

6.3 Capacitors

The integral over time of the instant power sent into the magnetizing device is the total energy (Joule) needed to produce one magnetic pulse.

$$p(t) = u(t) * i(t) = 518 * \sin(2\pi 1000t) * 315 * \sin(2\pi 1000t - \frac{47\pi}{100}) \tag{6.22}$$

$$E(t) = \int_{0.24ms}^{0.74ms} 518 * \sin(2\pi 1000t) * 315 * \sin(2\pi 1000t - \frac{47\pi}{100})dt \tag{6.23}$$

$$E(0.24 - 0.74ms) = 26.1J \tag{6.24}$$

The voltage drop at the dc-link is allowed to fall from 540V to 518V at a magnetic pulse.

To receive the value needed at the capacitors, these equations will be calculated:

$$E(t) = \frac{1}{2} * C(U_{DCLink}^2 - \hat{u}^2) \tag{6.25}$$

$$C = \frac{2 * E}{(U_{DCLink}^2 - \hat{u}^2)} = \frac{2 * 26.1J}{(540^2 - 518^2)} = 2.3mF \tag{6.26}$$

However, consideration of a safety margin is necessary and that will result in a higher value. At this point it is not decided, but it will probably be at about 3mF. To smooth up the operations of the capacitors and get a quicker response at the pulse, there will be mounted four capacitors. Two parallel circuits with two capacitors in each. It results in four capacitors with 3 mF and 300 V since the DC-link voltage is approximately 600 V.

Power loss calculations for the capacitors:

$$P_C = Q * \tan\delta = 315A * \left(\frac{1}{1000}\right) * \tan\delta \tag{6.27}$$

Where δ is the power loss factor, which is stated in the data sheets for the capacitor.

Normally the power losses over a capacitor is negligible, therefore no cooling system will be needed.

6.4 Three-phase rectifier

To calculate the necessary amount of current that the rectifier is subdued to deliver, the power is a necessary parameter to receive. With the amount of energy (eq.5.24) insertet in eq. 6.28, the poweramount is calculated. The pulse time is the halfed periodtime at one pulse.

$$P = \frac{E}{pulsetime} = \frac{E}{0.74 - 0.24ms} = \frac{26.1J}{0.5ms} = 52200W \tag{6.28}$$

The rectifier has to deliver at least 52200 W to the system.

Demands for current delivery from the power system

$$I_{powersystem} = \frac{\left(\frac{52200W}{3(phase)}\right)}{400V} = 43.5A \tag{6.29}$$

and for rectifier current

$$I_{rectifier} = \frac{P}{V_{dc,shot}} = \frac{52200W}{518V} = 101A \tag{6.30}$$

with

$V_{dc.magnetic\ pulse}$ = lowest permitted dc-link voltage (Further explained in section 8.1.1).

This is a maximum value of the power for the magnetizing device. However, the rectifier is not supposed to deliver all the energy for one magnetic pulse at the pulse

time. The energy is stored at the capacitors. A magnetic pulse will be performed at minimum every ½ second depending on that the synchronous motor has to adjust to a new position; this will substantially decrease the current.

$$P = \frac{E}{s} = \frac{26.1}{0.5} = 52.2W \tag{6.31}$$

$$I_{rectifier} = \frac{P}{V_{dc,shot}} = \frac{52.2W}{518V} = 0.1A \tag{6.32}$$

To slow down the current rush to the capacitors from the rectifier immediately after and during a magnetic pulse, a coil will be assembled between those components. This will also give a smoother DC-link voltage.

The selected rectifier is from Semikron, SKD 33.

6.5 Protective coil

The protective coil inductance is calculated from some stated parameters. The voltage over the coil will have a maximum value (V_{max}). Depending on the given voltage at the three-phase system at the rectifier and the voltage at dc-link ($V_{dc,magnetic\ pulse}$) right after a magnetic pulse is fired. The capacitors will be charged with energy corresponding to 518 V at this time and the highest voltage at the rectifier at any time are the power system top value 565V. Further, the current that is allowed to pass the coil is A_{max}. This limit arises from the rectifier limit that is 33A, approximated for safety reasons to 30A. The frequency after the rectifier is 6 times higher than net frequency.

$$V_{\max} = 565 - V_{dc,shot} = 565 - 518 = 47V \tag{6.33}$$

$$X_L = \frac{V_{\max}}{A_{\max}} = \frac{47V}{30A} = 1.6\Omega \tag{6.34}$$

$$f = 6 * 50Hz = 300Hz \tag{6.35}$$

$$L = \frac{X_L}{\omega} = \frac{1.6}{\omega} = \frac{1.6}{2\pi f} = \frac{1.6}{2\pi 300} = 0.83mH \tag{6.36}$$

For safety reason and securing that the current won't exceed a limit of 30 A, the wire must have a minimum resistance of 1.6 Ω. This is a necessary step of caution to eliminate the current rush when the voltage transient across the coil reaches its minimum value.

Voltage and current over a coil has the following functions and from the plot (*figure 6.2*) it is seen that whenever a magnetic pulse is fired the current wont exceed 30 A. Instead the current goes to zero immediately after a pulse and slowly increases. However, there will also exist a frequency of 300 Hz after the rectifier, which also decreases the current to the capacitors until they are fully charged.

$L = 0.83mH,$

$R = 1.6\Omega$

$I = 47/R = 30A$

$s = L/R = 0.5ms$

$u = 47 * e^{-t/s}$

$$i = I * \left(1 - e^{-t/s}\right) = 30 * \left(1 - e^{-t/s}\right) \tag{6.37}$$

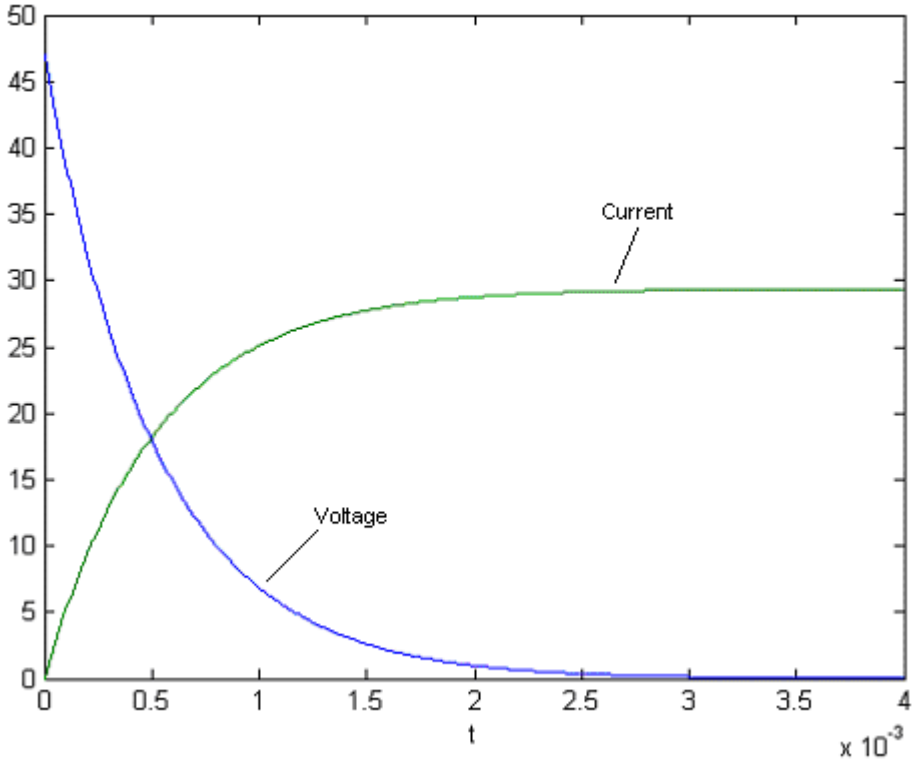

Figure 6.2: Voltage and current across the coil.

6.6 Heat sink

For calculations of the necessary cooling requirements a parameter (R_{thha}) needs to be found. This parameter is the factor for heat transfer from the component to the ambient air at the cooling element.

$$R_{thha} = \frac{T_h - T_a}{\sum_{i}^{n} P_{d,i}} \tag{6.38}$$

n=amount of components

$P_{d,i}$ = power loss at component i

T_a = temperature at ambient air

T_h = temperature for component at cooling element

The component that requires the lowest temperature at the cooling element will place the boundary at the transfer factor.

Maximum working temperature for diode (T_{Dj}) respectively transistor (T_{Tj}) is 150°C.

The rectifier does not need any cooling device.

$$T_h = T_s = T_j - P_{d,i}(R_{thjc} + R_{thcs} + R_{thjs}) \tag{6.39}$$

$$T_{hT} = T_{sT} = T_{jT} - P_T(R_{thjc} + R_{thcs}) = 150 - 1295(0.055 + 0.038) = 29.5°C \tag{6.40}$$

$$T_{hD} = T_{sD} = T_{jD} - P_D(R_{thjs}) = 150 - 672(0.125) = 66°C \tag{6.41}$$

$$T_h = \min(T_{h,i}) = T_{hT} = 29.5°C \tag{6.42}$$

$$R_{thha} = \frac{T_h - T_a}{\sum_i^n P_{d,i}} = \frac{29.5 - 25}{1295 + 672} = 0.002\frac{K}{W} \tag{6.43}$$

The air-cooled element does not fulfill the demands for this low transfer factor. Instead the cooling device has to be water-cooled.

$$T_a \Rightarrow T_{water} = 10°C$$

$$R_{thha} = \frac{T_h - T_{water}}{\sum_i^n P_{d,i}} = \frac{29.5 - 10}{1295 + 672} = 0.01\frac{K}{W} \tag{6.44}$$

Suitable cooling element will be WP 16/270 at Semikron, with R_{thhw} (6 l/min) = 0.014. [5], p.2092.

7. Sensor

Measurement of the magnetic flux reminisce at the ring is performed by a hall sensor. A current is arising inside the Hall effect sensor due to the magnetic flux density at the ring. This sensor is placed at distance of 0.5 mm from the ring. The generated signal from the sensor is in voltage.

The sensor is a linear hall effect sensor, A3515LUA.

8. Control system

To make the regulator it is necessary to measure the current through the coil at any time. This is done with a coil placed around the wire that transfers current to the magnetizing device. Since the inductance of the coil at the magnetizing device is very well defined it is used to calculate the amount of voltage needed across the coil.

$$U_{coil} = L * \frac{di}{dt} \tag{8.1}$$

$$L = 0.27mH$$

$$\frac{di}{dt} = \omega\hat{i} * \cos(\omega t - \varphi) = 2\pi 1000 * 315 * \cos\left(2\pi 1000t - \frac{47\pi}{100}\right) \tag{8.2}$$

$$U_{coil} = 0.27mH * 2\pi 1000 * 315 * \cos\left(2\pi 1000t - \frac{47\pi}{100}\right) \tag{8.3}$$

The figure 8.1 shows the relationship between the three parameters Voltage, Current and magnetic flux at a pulse.

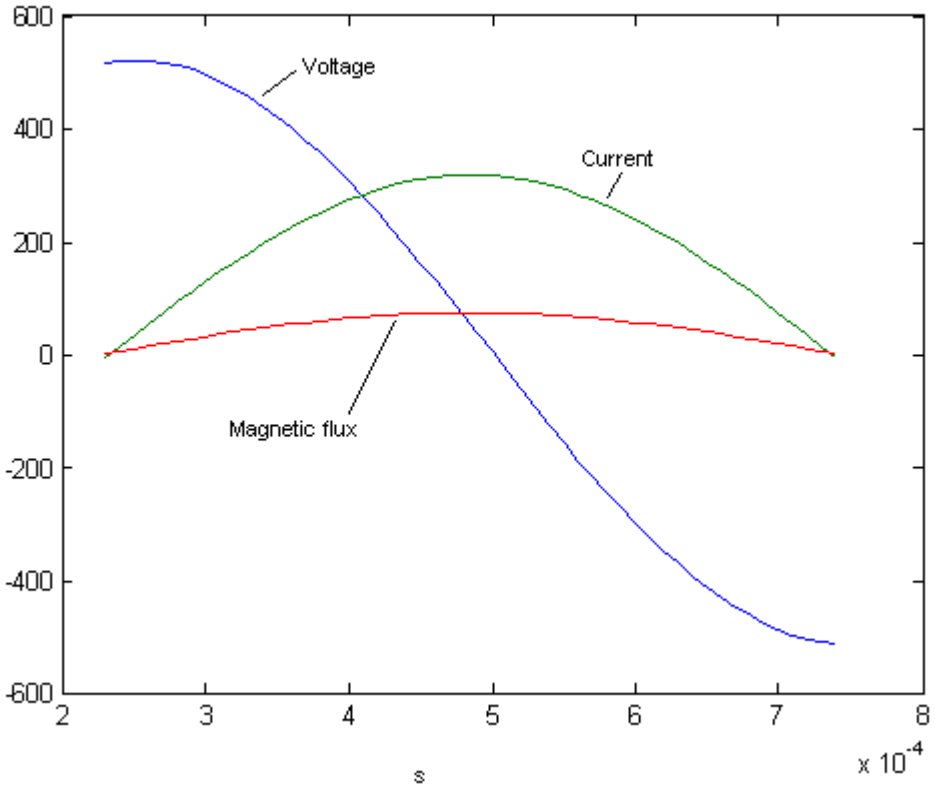

Figure 8.1: The controlled parameters.

8.1 Control simulation

The control of the magnetizing device is tested in simulation with Simulink. It consists of an inner and an outer control loop. The inner loop control the voltage across the coil and the outer loop control the current. The reference signal is set to be the current. This is intended to be an adaptive control and therefore the control program will change this signal as the process is progressing. The current reference signal will be the origin of the voltage reference signal. The voltage is calculated by assistance of the above stated equations. Voltage reference is set to be across the coil of the magnetizing device, therefore the voltage drop across the built-in resistance is subtracted from the output voltage signal to the coil.

The limitation for the output voltage is the capacitance discharge voltage. As the pulse is progressing the capacitances are discharged, which comply with a dc-link voltage drop. The dc-link voltage is the maximum voltage that can be achieved across the coil and the built-in resistance. However there will be a minor charge current from the rectifier at the pulse, but it will be fairly small due to the emplacement of an protective inductance between it and the capacitors, so that charge current will be neglected in this model.

The Zero order hold block is intended to simulate the sample and hold at the input signals to the computer control. This delay could have a minor consequence at the control signals. The simulation model is shown in figure 8.2. Figure 8.3 shows the sub system with the voltage limiter at dc-link that will decrease the dc-link voltage while a magnetic pulse is performed.

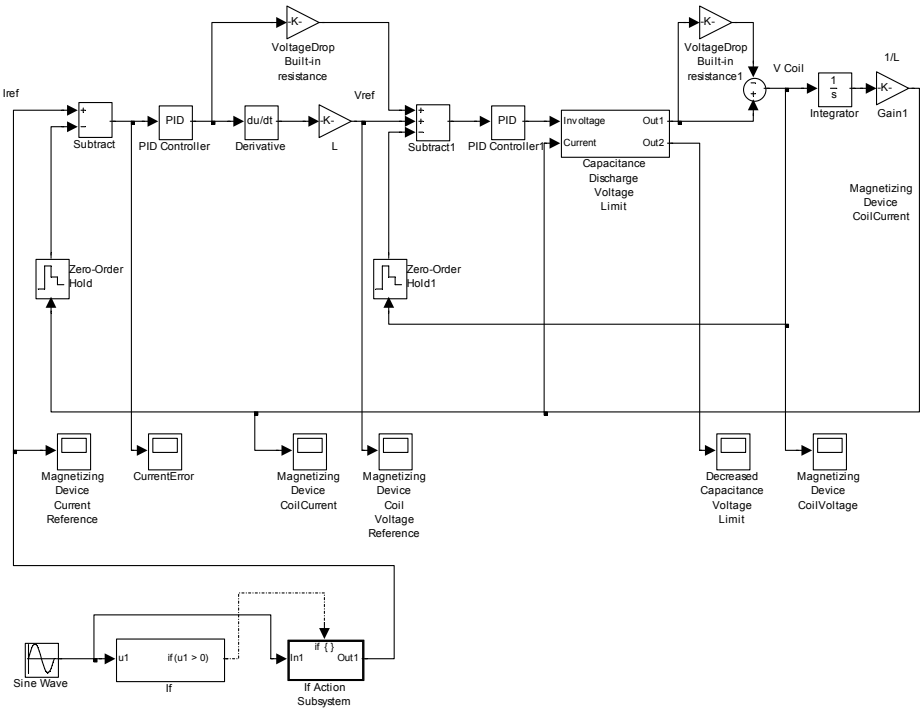

Figure 8.2: Simulation model.

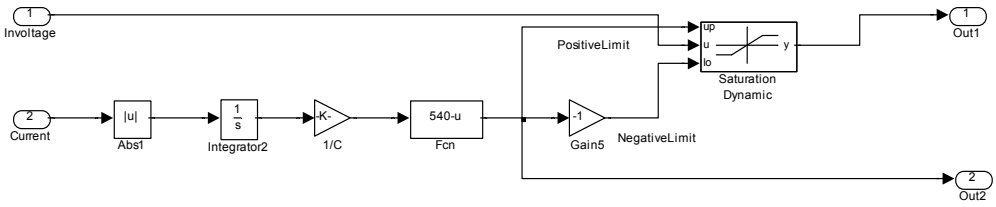

Figure 8.3: Subsystem; Capacitance Discharge Voltage Limit.

The simulation shows that the capacitance is large enough to hold the minimum permitted dc-link voltage. The capacitance has been raised to the level of 4mF. With 3mF the voltage decreased until 505V and that is acceptable as well. The reason for increasing the capacitance is due to the availability for those capacitances at the lab.

The current is hold with satisfaction and it can be seen that the voltage limit will go as low as 515V. However, this does not affect the voltage demand at the coil. There is a voltage spike at the start of the pulse and this will raise the current very fast, so the voltage will therefore be low for the rest of the pulse.

At this plots (*Figure 8.4*) there is a large integral gain at the outer loop (Current signals). In the simulation there is proportional gain and integral gain. Derivative gain is left out due to the high switching frequency at the IGBT:s. The noise will exclude the opportunity to use derivative gain from the controller.

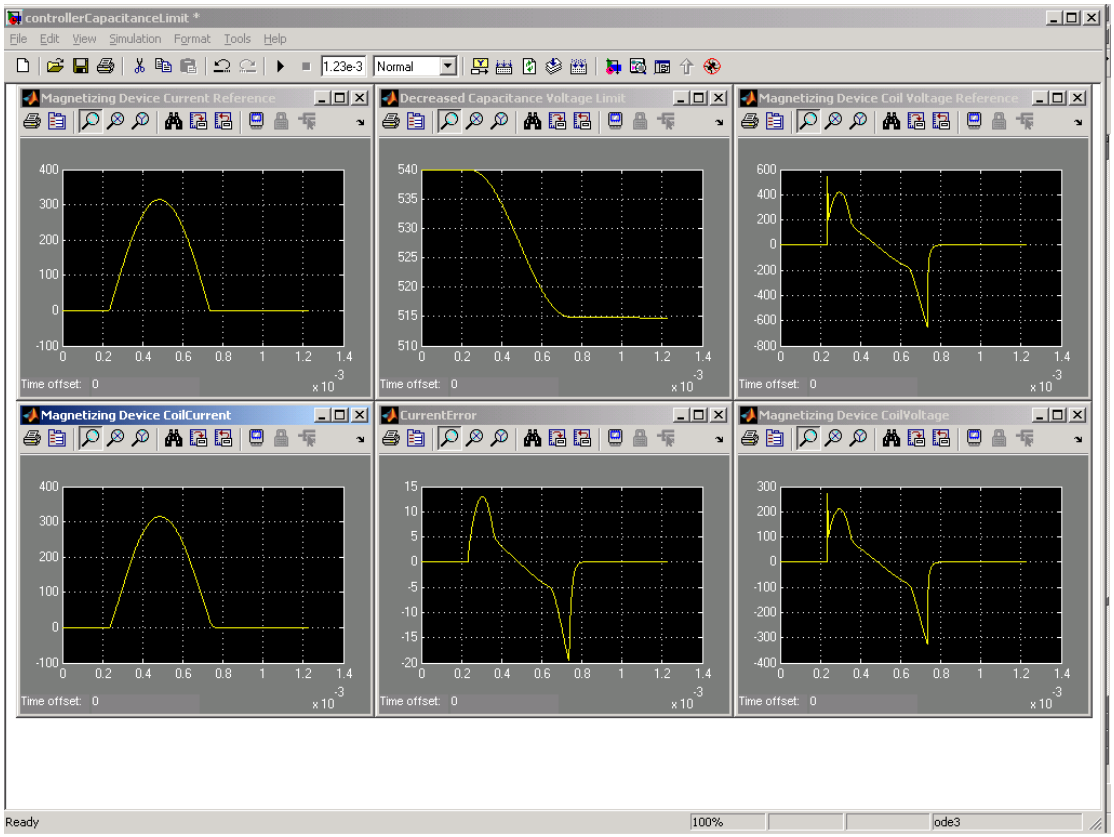

Figure 8.4: Plots for the simulation.

8.1.1 Voltage limit calculations

The sub system contains the parameters for calculation of the voltage limit. At the start of a pulse there are 540 $V_{DC\text{-}link}$. As the current pulse is advancing the charges is leaving the capacitors. To calculate the voltage limit along the pulse there are some equations that has been used.

$$C = \frac{Q}{V_{Capacitor}} \tag{8.4}$$

$$Q = i(t)\int_0^t dt \tag{8.5}$$

$$V_{Capacitor} = \frac{i(t)}{C}\int_0^t dt \tag{8.6}$$

$$V_{DC.link} - V_{Capacitor} = V_{Limit} = 540 - \frac{i(t)}{C}\int_0^t dt = 540 - \frac{i(t)}{3mF}\int_0^t dt = 540 - \frac{i(t)}{3mF}t \tag{8.7}$$

The $V_{DC\text{-}link}$ is the voltage at the start time at the dc-link and the $V_{Capacitor}$ is the voltage amount that has been taken out from the capacitors along the pulse.

8.2 Real control device

The voltage reference signal has to be halved at the real model. The cause is that the voltage between the two IGBT half bridges must have the $V_{DC\text{-}link}$ when conducting. One of the V_{Ref} signals will also change polarity to negative sign. The positive reference will be the upper one and the negative the lower reference level.

When switching occurs at the control system this will lead to a voltage at the magnetizing device that corresponds to the whole voltage reference signal.

The switching will be performed by calculation of percentage times that the IGBT:s will be opened. This will result in a PWM (Pulse Width Modulation) signal that set the on and off times for the IGBT:s. Figure 8.5.

The program for controlling the power electronics is done in Simulink and the reference input signal is the current. This signal is a sine wave; therefore the voltage reference will have the same properties.

To be able to simulate the model or alternately using the model in real time with dSpace, there exists two manual switches. Those switches can be switched to perform the wanted execution.

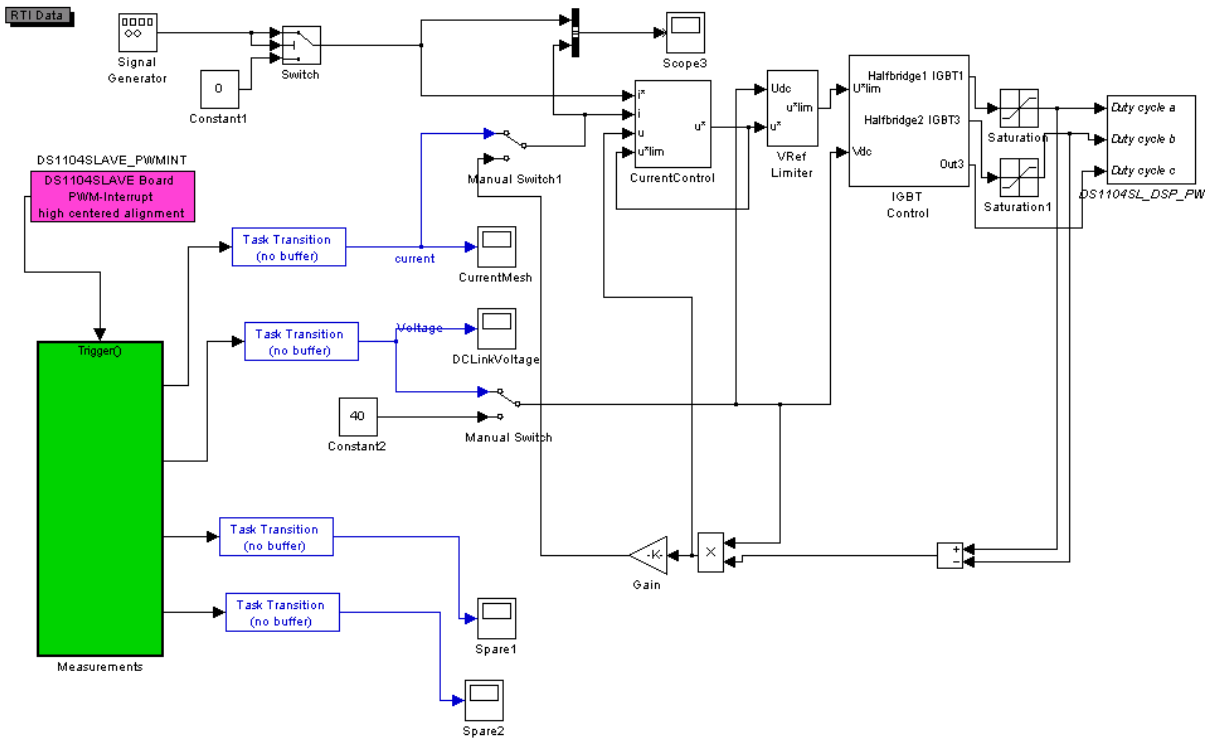

Figure 8.5: Simulation model.

There are two measured signals; the dc-link voltage and the current through the magnetizing device. Those signals are trigged to measure when the PWM signal is on the centre at its peak value. This gives a satisfying value similar to an average value when the current has risen by half for each switching. Figure 8.6.

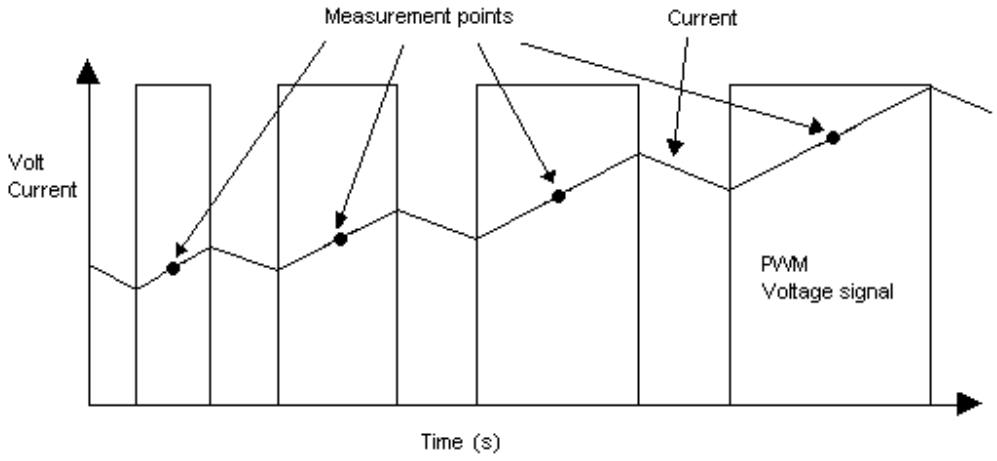

Figure 8.6: Triggered measurement points.

Inside the measurement block is the in signals represented as ADC (Analog/digital Converter) block, which are shown in figure 8.7. Those blocks sample the signal and transfer it to signals represented in zeros and ones that the computer is able to read.

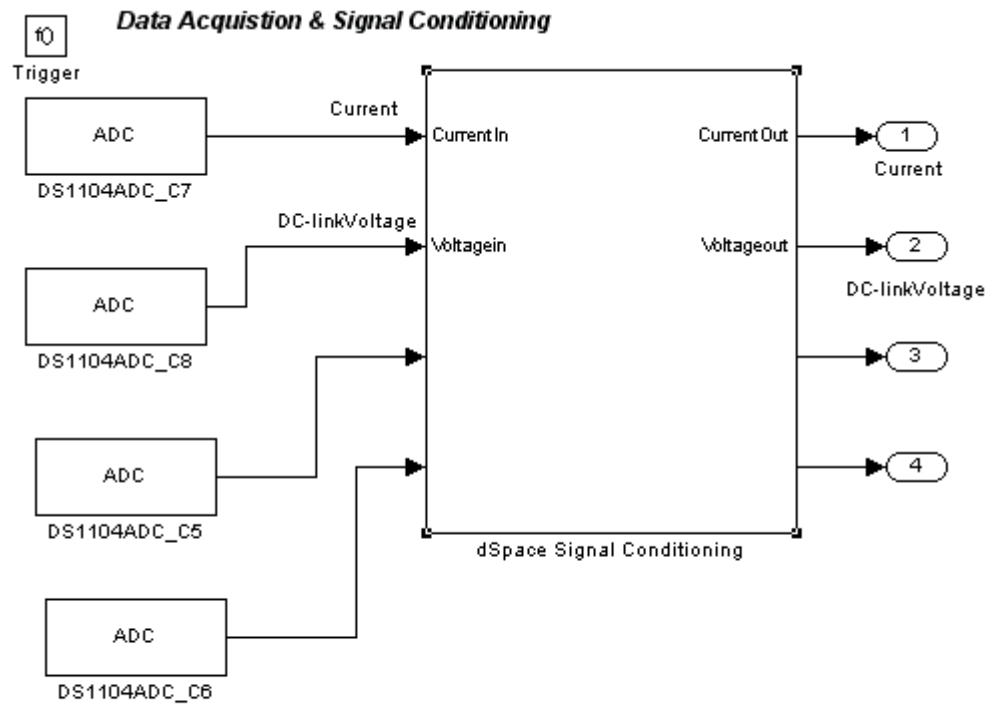

Figure 8.7:Measurement block.

Gain block adjusts the measured signals to correspond to the right amount of dc-link voltage respectively current. Figure 8.8.

Adjustment:

$$\text{Current}(\text{Current}_{\text{measured}}) = 10.4142857 * \text{Current}_{\text{measured}} - 0.2403333$$

$$\text{dc-linkVoltage}(\text{dc-linkVoltage}_{\text{measured}}) = 2015.53571 * \text{dc-linkVoltage}_{\text{measured}} - 1041.7767$$

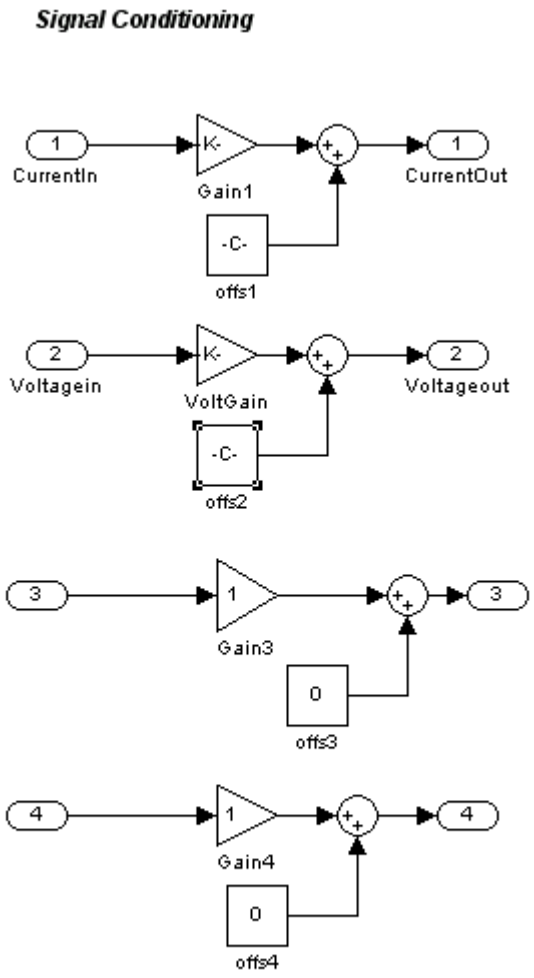

Figure 8.8: Adjustments.

Current control consists of a PI controller and compares the measured current at the magnetizing device and subtracts this signal from the current reference. This leads to that the controlling only will be performed at the current error. The voltage reference is calculated by the program and used for controlling. To ensure that a large error won't give raise to wind up at the controller, there's an anti wind up part. This decreases the integral part when the reference signal is greater than the dc-link voltage. Otherwise this could lead to a large overshoot at the current threw the magnetizing device, due to a stored error at the integral part. Figure 8.9.

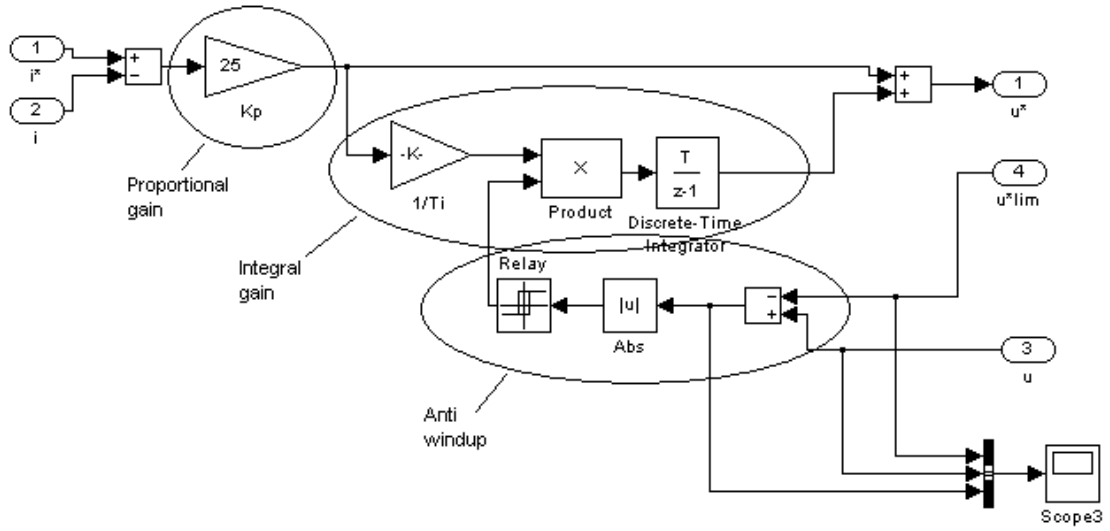

Figure 8.9: Current control block with anti windup.

The voltage reference is sent to the VRefLimiter, which set the boundary at the voltage to the dc-link voltage. Due to the impossibility to control with a voltage, that doesn't exist. Figure 8.10.

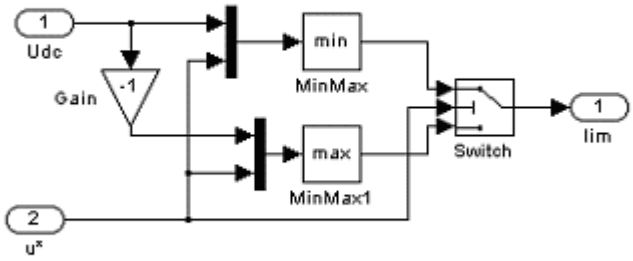

Figure 8.10: VrefLimiter block.

The IGBT Control block sets the percentage for opening the IGBT:s halfbridges, where the offset is 0.5 (50%). Those signals is sent to IGBT1 and 2, the inverse is sent (with dSpace) to IGBT3 and 4. When both half bridges get the offset signal it corresponds to zero voltage across the magnetizing device. Figure 8.11.

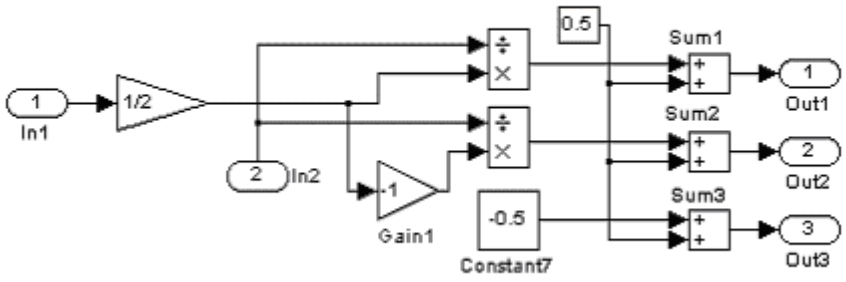

Figure 8.11: IGBT Control block block.

To ensure that the percentage wont exceed 100% respectively fall below 0%, there is two saturation blocks that are set to 1 respectively 0.

The simulated signals are shown in figure 8.12, the current reference signal and the current threw the magnetizing device. It works with full satisfaction in a simulation.

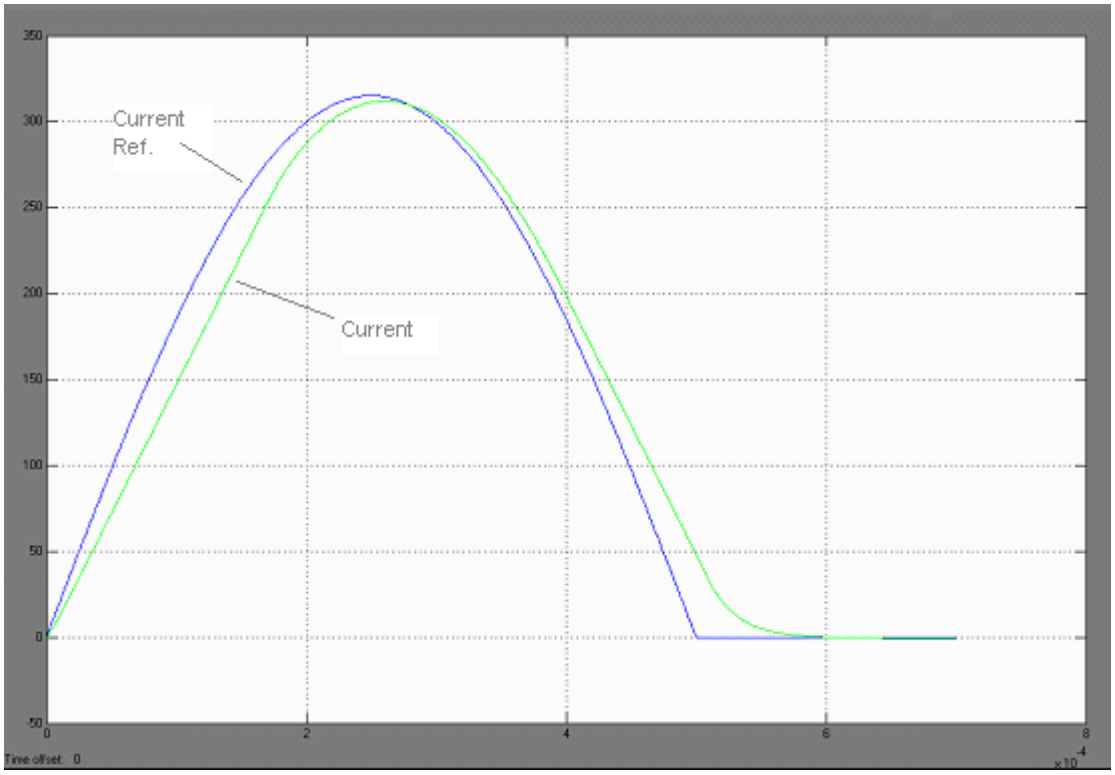

Figure 8.12: Current measurements at simulation.

8.2.1 dSpace

To handle the I/O-signals a program called dSpace is used. This will sample the in signals respectively send signals for the IGBT:s to conduct. The PWM signals for the IGBT:s will have the values 10V respectively 0V for on and off. For the sensors the analogue signal varies between 10V and 0V. Those signals are A/D converted to the computer.

8.3 Connections

Signals from the outer system to the computer respectively the signals from the computer are represented in this section.

8.3.1 In/Out-signals

The I/O-signals have to be buffered through a PCB-board before they are sent to respectively device. They have to be galvanic separated. However, the current measurement signal will not pass a PCB-board constructed in this thesis. Instead it will transfer via a ready mounted rectifier board. The voltage measurement use a separated board, cause to the high voltage measurement signal. This along with the frequency would otherwise affect the on/off signals to the IGBT:s with an unacceptable high noisy environment. The signals are represented in table 8.1, seen from the PCB-board.

Utilization	From device/Pin	In value	Out value	To device/Pin
On/Off for IGBT1 to 4.	dSpace, PWM signal.	10, 0V	15, 0V	Driver card 1 and 2/ X1.4, X1.2.
Voltage measurement across coil.	Voltage transducer, LV 25-P, LEM module/M.	0-25mA	0-9V	DSpace, ADC
Reminisce of Magnetic flux at ring.	Hall/3.	0-8V	0-8V	DSpace, ADC
Current measurement thru coil.	Current transducer, HA 500SB, LEM-module/White cable.	Not on PCB	Not on PCB	DSpace, ADC

Table 8.1: Signals representation.

8.3.2 PCB buffer board layout

The layout is developed in a cad program and then converted to an overhead film for etching on a double plated PCB-board.

The IGBT:s on/off signals are buffered through a comparator cause to the demands for fast response times. The used comparator is the LM339N. Pull up resistors for the exit as well as stabilizing resistors at the entrance is used with the value 2kΩ. The negative entrance at the comparator has an offset of 2V. due to the high sensitivity to the noise at the gates on the PCB-board. This slows down the response time and could be lowered to approximately 1V to minimize this affect. However, it is important to

exclude that the IGBT:s could get on signals at the same time. This event will otherwise trig an error signal and block the IGBT:s.

At the same board there are two error signals for the drivers. When there's an error at the driver, a red LED-diode will light cause to a transistor is opening inside the driver card. Those errors are reset with a switch that set the value 0V at the both on/off entrance at the driver. The switches are not shown at this picture. Figure 8.13.

There's also the detection of magnetic flux reminisce at the ring on this board. It consists of a follower that tracks the in signal sent from a hall sensor. This varies between 0 and 8V.

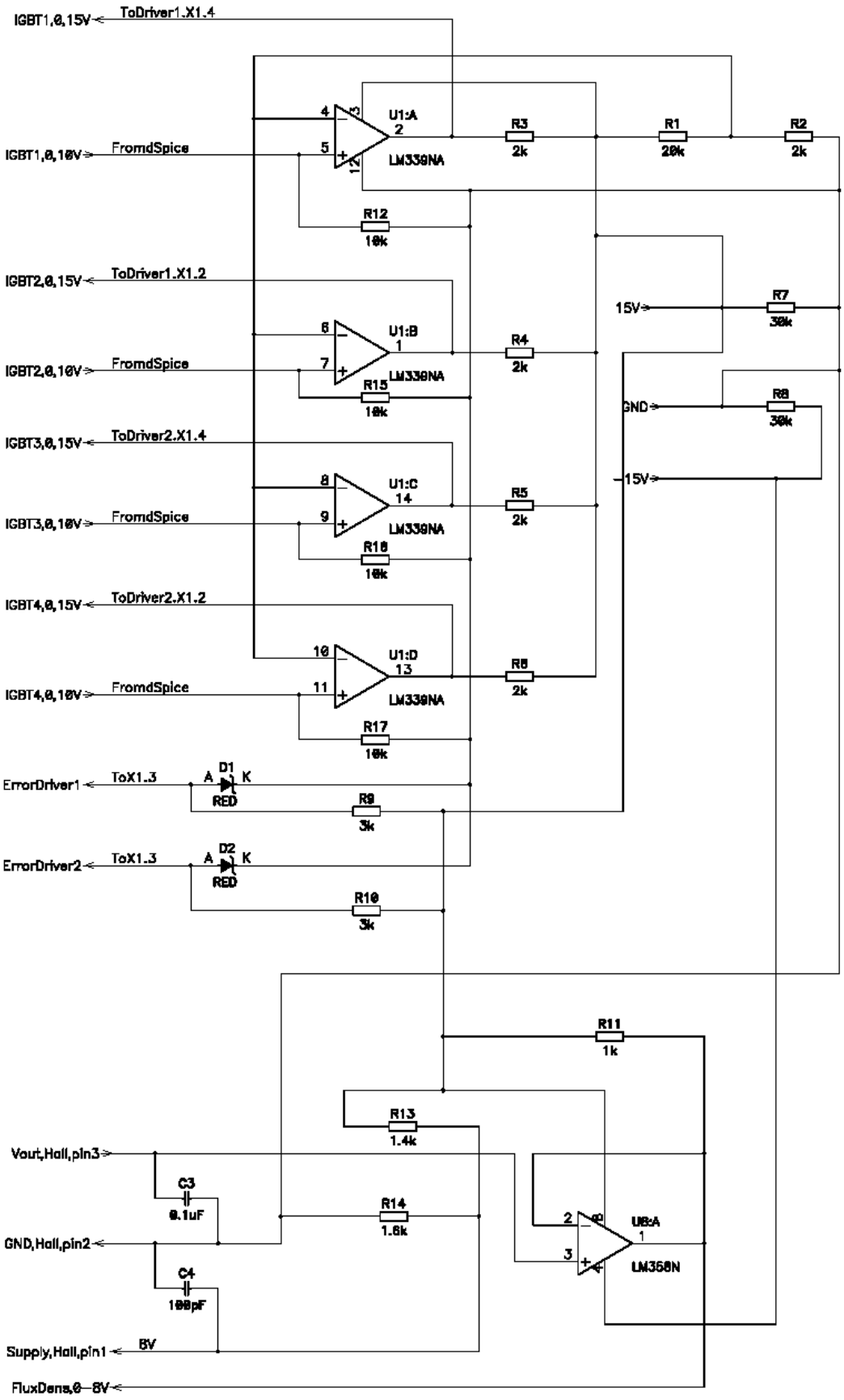

Figure 8.13: Drawing for PCB-board.

Voltage measurements are mounted on a separated board that is encapsulated in a metallic shield. Figure 8.14. The variable resistor (R3) is used to adjust the offset at the sensor. Resistor R4 and R2 sets the offset at approximately 5V. This module is adjusted to meet the demands for measurements between 540V and –540V. It sends a signal between 9V and 1V.

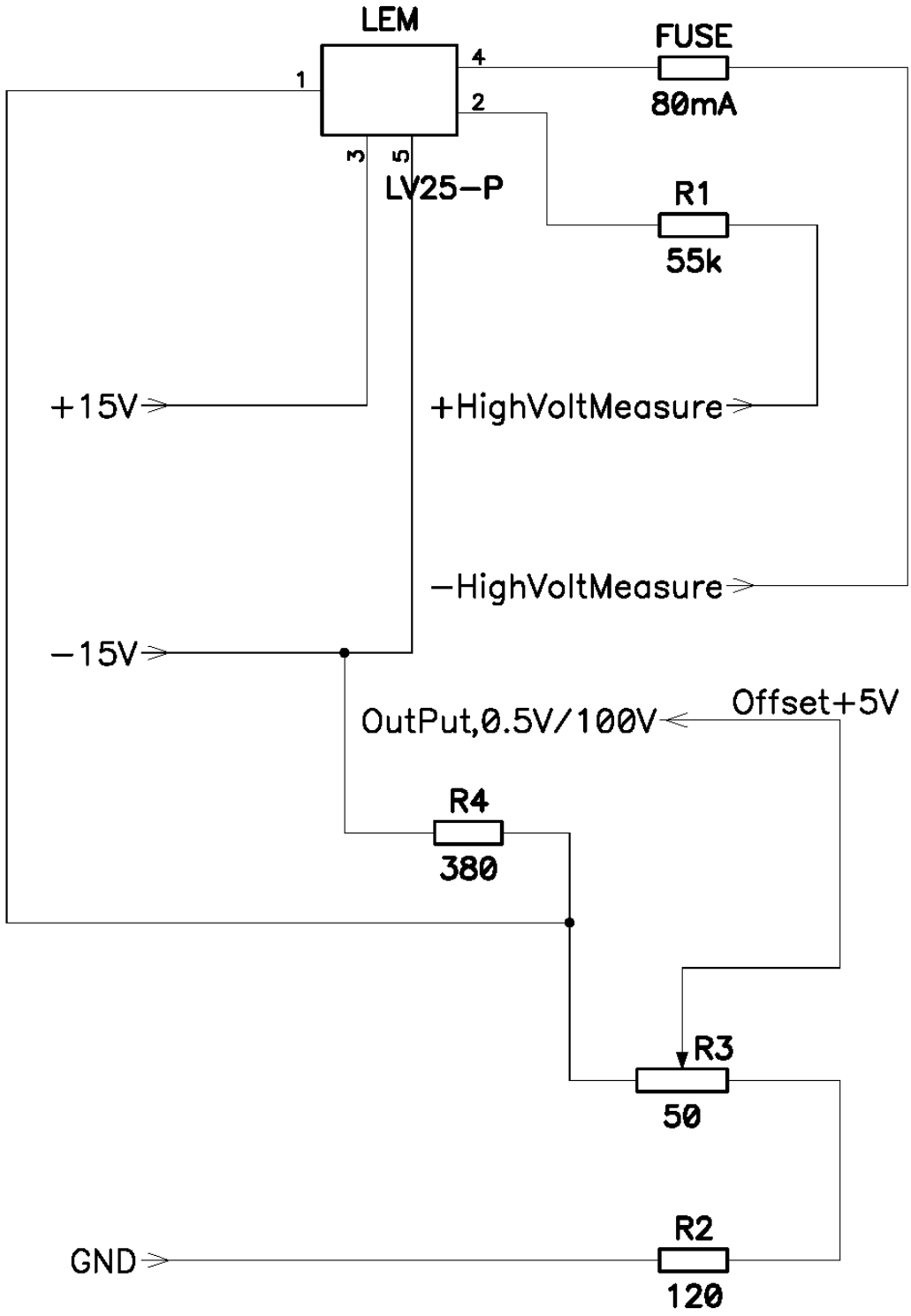

Figure 8.14: Voltage measurement.

The finished buffer board is seen in figure 8.15. The alternating switches set the reset value 0V for the drivers to reset the error. Much of the copper is remained solid due to

minimize the noise. These thick lines are covering the back of the board as well and they are connected to the ground level.

To the right is the voltage measurement board. It is encapsulated in a metallic shield, as mentioned in section 8.3.2. The high voltage side are also separated from the out signals cause to noise minimization. High voltage side is the upper region on the board.

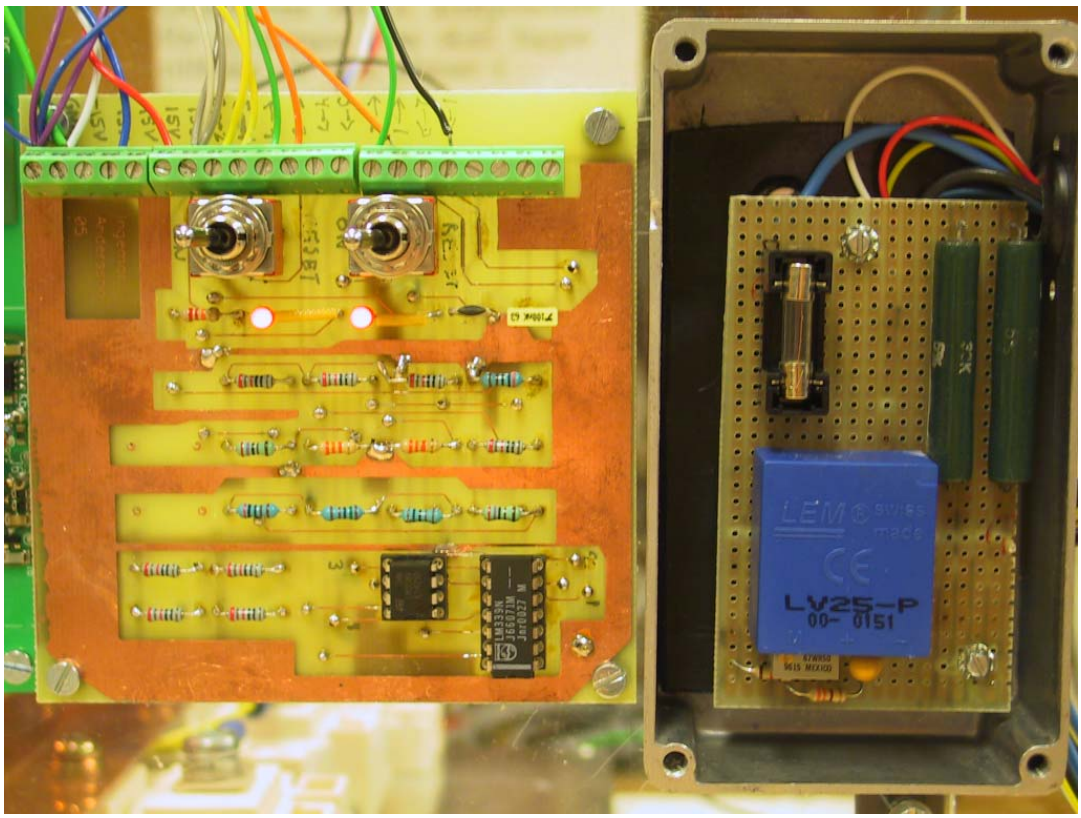

Figure 8.15: Buffer board and voltage measurement.

9. Built Model

The result for the thesis so far is a built four-quadrant converter. *Figure 9.1-2*. It has the PCB-boards mounted on the side to be easily reachable. Touching them at the operation is fairly safe. The plastic glass is a borderline for safety. Behind this are the dc-link copper plates that are paralleled to obtain capacitance properties. This decreases the inductive behaviour of the dc-link. There are mounted resistors of 20kΩ parallel to the capacitors to slowly discharge them at operation shut off. Otherwise they would be fully charged after shut off which have highly dangerous consequences.

The IGBT:s are placed right over the water pipes at the cooling device to receive maximum cooling. Pipes are coming out on the both sides at the model, in this way there are no unnecessary crossings between water and electrical devices.

The rectifier is placed at the cooling device beside the IGBT:s to get out of the way for the load.

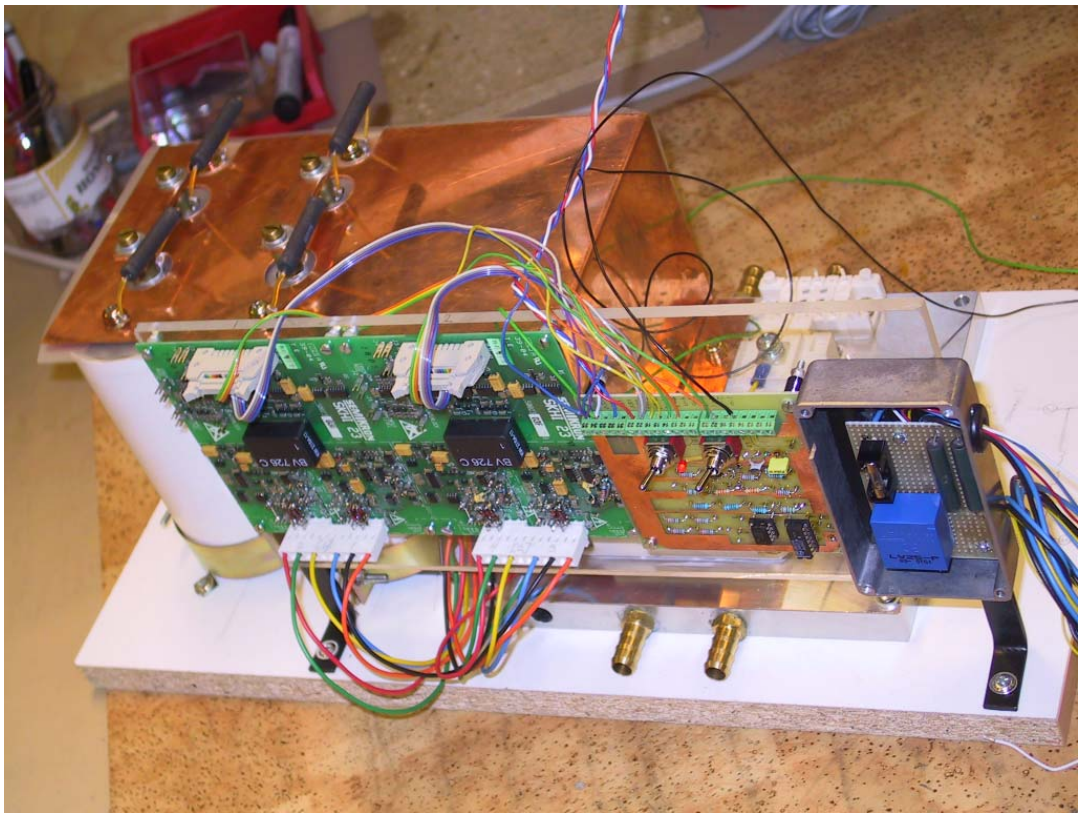

Figure 9.1: Four-quadrant converter.

Figure 9.2: Four-quadrant converter.

9.1 Switching behaviour

Figure 9.3 shows the delay time for the comparator at the buffer board. It can be seen that it is only approximately 270ns. The datasheets for the comparator LM339N expresses a delay time for 0.3µs, with is the time from 10% of the in signal to 90% of the out signal. It can also be determined from the figure.

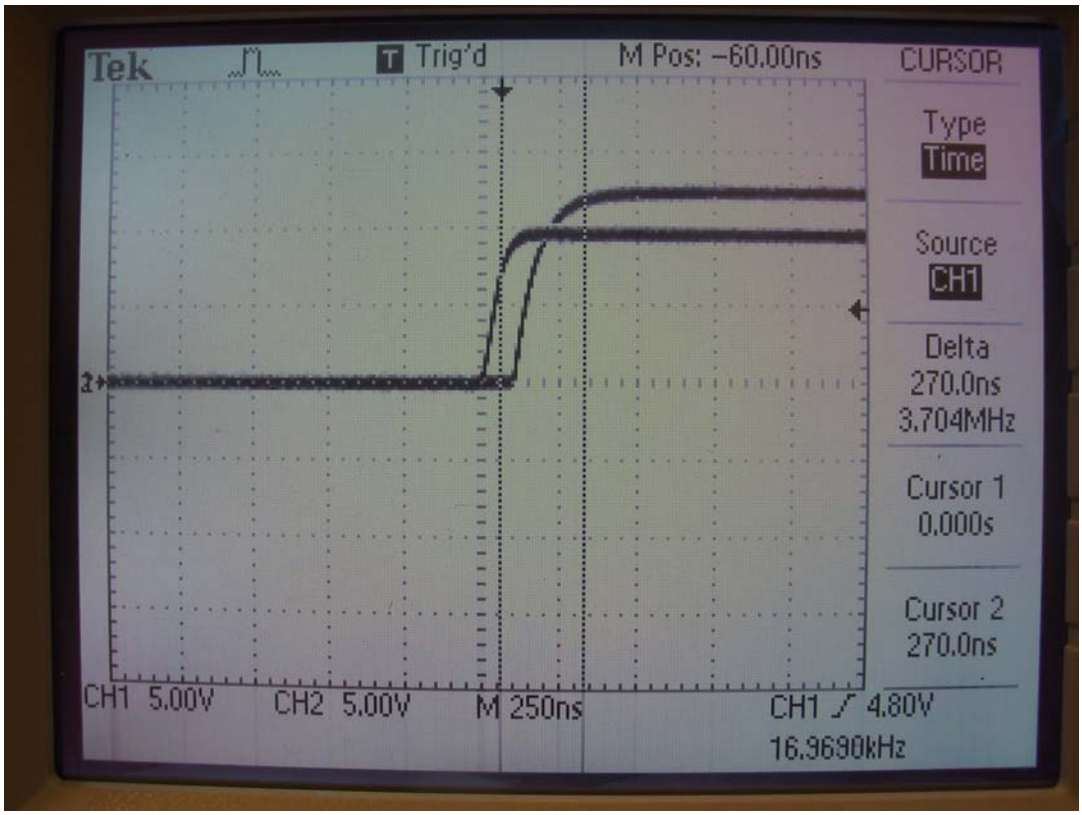

Figure 9.3: Delay time for the comparator LM339N.

The delay time for the driver is shown in figure 9.4. And it is fairly high in comparison to the buffer board delay time. The driver has a delay time of approximately 2.2µs. The value is 1.4µs at the data sheet for the driver SKHI 23/17.

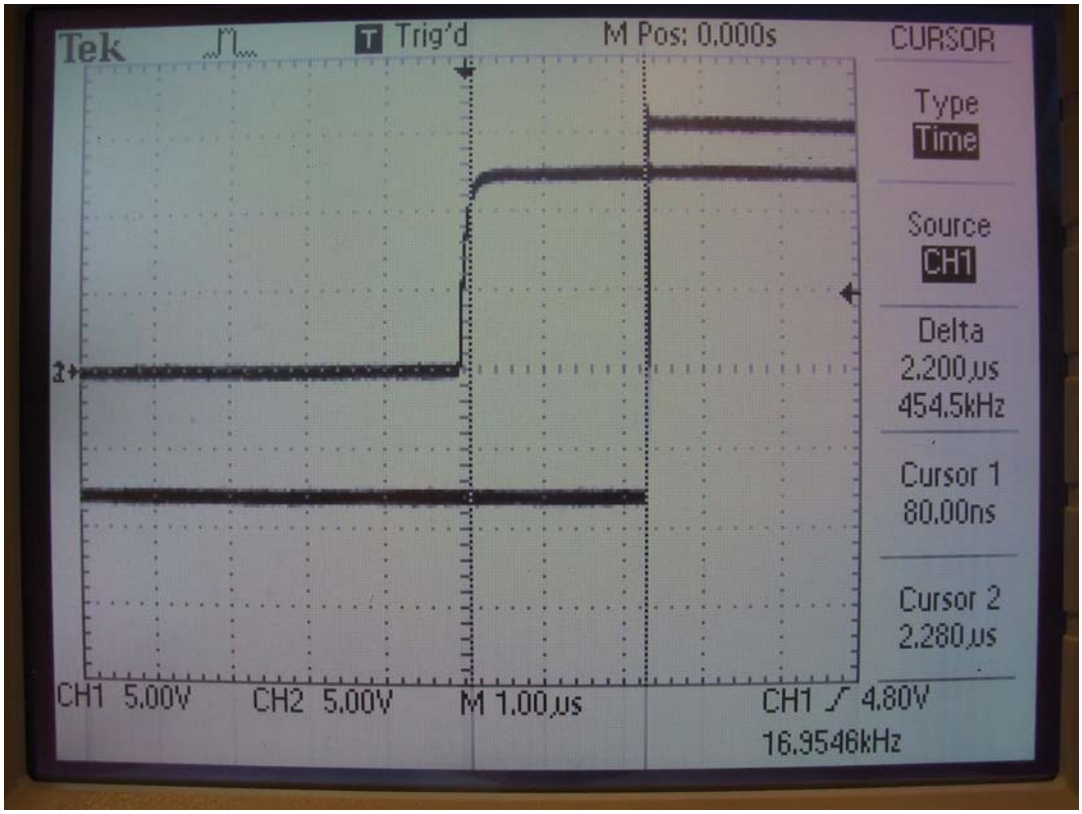

Figure 9.4: Delay time for the driver SKHI23/17.

10. Conclusion

This thesis has not been finished in the given time. This is due to the delivery times for the different materials as well as practical problems. The simulation and calculations is always viable and straight forward to do, while the real testing isn't always that straightforward. I have earned a lot of experience on the way to the enclosure of this thesis, especially at the construction part.

So far this thesis has lead to the completed building of a four-quadrant converter. The initial switching test of the drivers is completed and it is switching with satisfaction. The IGBT:s is performing the wanted switching behaviour and the regulator is working properly.

Programming for the magnetic flux measurement and the synchronous motor as well as the building of a magnetizing device has to be performed. The magnetizing device is not build at the university.

11. References

[1] Ola Andersson. High velocity compaction of software magnetic composites. Höganäs AB, Sweden.

[2] Håkan Skarrie. Design of Powder Core Inductors. Licentiate Thesis. Department of Industrial Electrical Engineering and Automation. Lund University.

[3]Per Karlsson. Kraftelektronik. Industriell elektroteknik och automation. LTH. Oktober 1998.

[4] Dr. Peter Campbell. Magnet design. http://www.magnetweb.com/.

[5] Semikron. Power electronics. 2004.

[6] http://hyperphysics.phy-astr.gsu.edu/hbase/hph.html

[7] Joseph J. Stupak Jr. Methods of magnetizing permanent magnets. Oersted Technology Corporation. Oktober 2000.

[8] Toru MAEDA, Haruhisa TOYODA, Naoto IGARASHI, Kazuhiro HIROSE, Koji MIMURA, Takao NISHIOKA and Akihiko IKEGAYA. Development of Super Low Iron-loss P/M Soft Magnetic Material. SEI TECHNICAL REVIEW · NUMBER 60 · JUNE 2005.